Table 2 The percentiles for patients with short QT interval

Percentile	Bazett QTc interval (ms)	
	Male	Female
100	362.0	369.0
99.5	362.0	369.0
97.5	362.0	369.0
90	362.0	369.0
75	361.0	368.0
50	359.0	366.0
25	355.0	362.0
10	349.0	355.4
2.5	340.6	345.9
0.5	331.2	329.0
0.0	331.0	329.0

very short QT intervals in both genders. There was a 1.8-fold male predominance in patients with very short QT interval. There are various underlying diseases, in which rate did not differ between short and very short QTc intervals in both genders. Figure 2 shows the age-specific prevalence of total, male, and female patients with short QT interval. The histograms generated according to the number of patients are shown in the upper row of Figure 2. The prevalence was biphasic in each group, with a higher prevalence in young and old adults and with a lower prevalence in middle-aged individuals. The prevalence showed comparable distribution when histograms were generated according to a ratio of patients with short QT interval to total patients in each decade (the lower row in Figure 2).

ECG characteristics of short QT interval

Table 4 lists ECG characteristics. There was no significant difference in various ECG variables between patients with short and very short QT intervals. AF was present in 23 of 234 (9.8%) male and 16 of 193 (8.3%) female patients (P = NS). The prevalence of AF did not differ significantly between patients with short and very short QT intervals in both genders. The prevalence of early repolarization was significantly (P = .0001) higher in 23 of 234 (9.8%) male than in 3 of 193 (1.6%) female patients, but was not significantly different between patients with short and very short QT intervals in both genders. In these patients, 11 (42.3%) exhibited early repolarization in anterior leads (V1-4); 9 (34.6%) patients in inferolateral leads (II, III, aVF, V5, 6); and 5 (19.2%) patients in anteroinferior leads (V1-4, II, III, aVF).

Long-term outcome

Long-term prognosis was assessed in 327 of 427 (77%) patients (182 men; mean age, 46.4 ± 22.3 years) with short QT interval. The mean follow-up period was 54.0 ± 62.0 months (range 1.1 to 299.8 months). In patients whose prognosis was evaluated, QT interval was 360.3 ± 24.8 ms and QTc interval was 359.8 ± 7.1 ms. During the follow-up period, 2 male patients developed life-threatening events. One patient was a 22-year-old man who exhibited early repolarization. This patient was admitted to our hospital because he suffered from syncope when drinking in 1989. There was nephritic syndrome in his past medical history, but no family history of cardiac disorders or sudden unexplained death. On admission, 12-lead ECG exhibited early repolarization in ECG leads corresponding to the inferolateral wall of the left ventricle (Figure 3). This patient revealed no evidence of abnormality of cardiac function and morphology by transthoracic echocardiography. Coronary angiography failed to find morphological abnormality, and coronary spasm was not induced by ergonovine injection. However, ventricular fibrillation occurred when the ECG recording was taken after hyperventilation. Because sinus bradycardia preceded the occurrence of ventricular fibrillation, orciprenaline sulfate (30 mg/day) was administered. Seven years later, the patient experienced a storm of ven-

Table 3 Clinical characteristics in patients with short and very short QT intervals

	Male			Female		
	Very short (≤355 ms, N = 65)	Short (356 to 362 ms, N = 169)	P value	Very short (≤360 ms, N = 36)	Short (361 to 369 ms, N = 157)	P value
Age (yrs)	43.6 ± 23.4	41.2 ± 20.8	.46	46.3 ± 24.9	45.0 ± 23.1	.77
Hypertension (N, %)	13, 20.0	31, 23.9	.54	10, 27.8	27, 26.7	.90
Angina (N, %)	6, 9.2	15, 11.5	.62	1, 2.8	12, 11.9	.08
Myocardial infarction (N, %)	4, 6.2	3, 2.3	.19	2, 5.6	1, 1.0	.14
Valvular disease (N, %)	2, 3.1	8, 6.2	.34	3, 8.3	7, 6.9	.78
Heart failure (N, %)	12, 18.5	22, 16.9	.79	6, 16.7	18, 17.8	.88
Arrhythmia (N, %)	19, 29.2	25, 19.2	.12	7, 19.4	15, 14.9	.53
Diabetes (N, %)	8, 12.3	23, 17.7	.32	4, 11.1	15, 14.9	.57
Dyslipidemia (N, %)	7, 10.8	22, 16.9	.24	6, 16.7	18, 17.8	.88
Follow-up (months)	42.1 ± 47.3	54.0 ± 64.6	.20	49.3 ± 65.7	49.7 ± 62.7	.98
Death (N, %)	3, 4.6	3, 1.8	.24	0, 0	0, 0	—
Ventricular fibrillation (N, %)	1, 4.2	0, 0	—	0, 0	0, 0	—

Arrhythmia involves patients with various types of rhythm disorders, except for patients who exhibited AF when the ECG was taken. Surgery indicates patients who underwent ECG recording before surgical procedure. Others includes patients who suffered various internal diseases or who were suspected to have a cardiovascular disease.

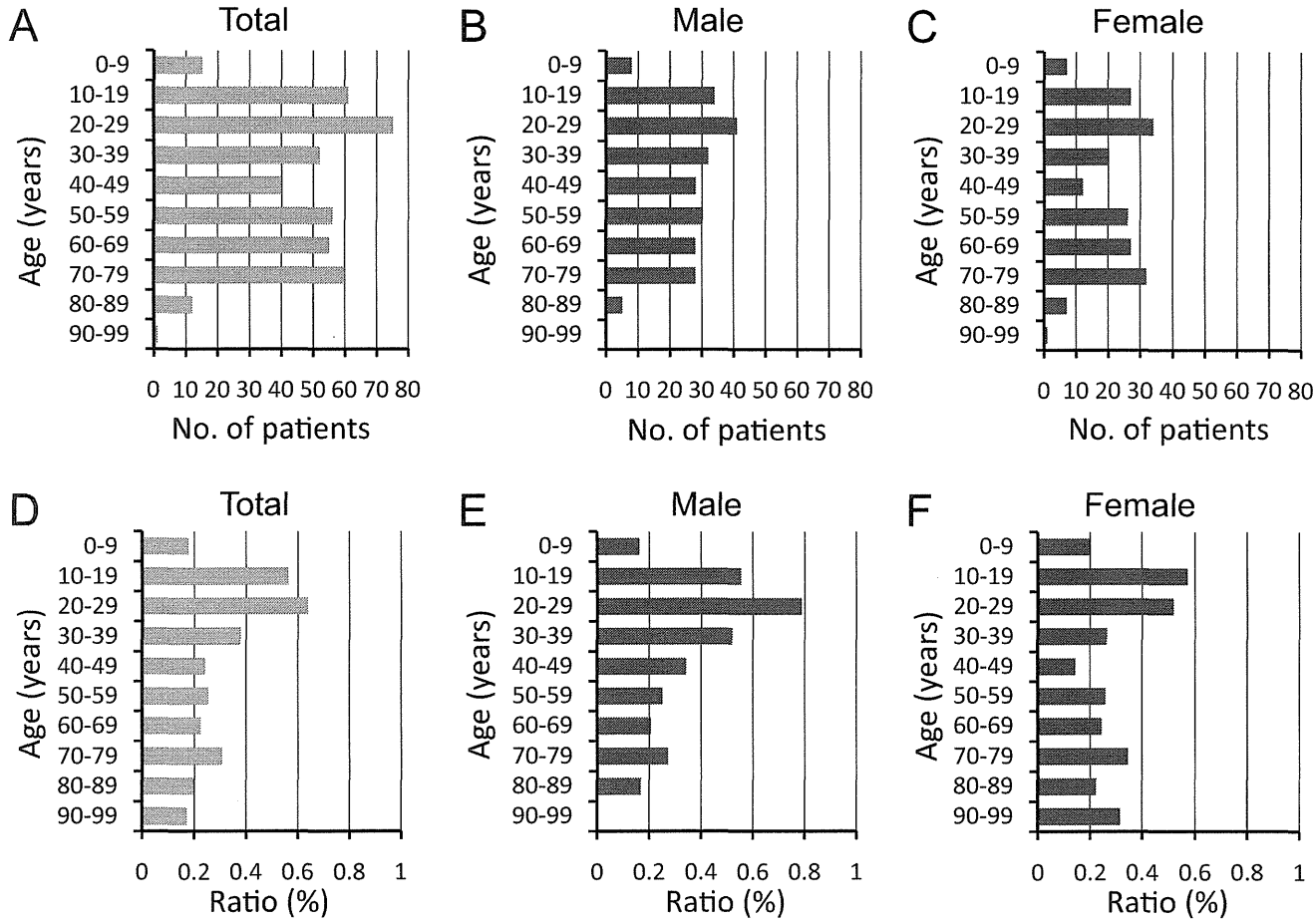

Figure 2 Age-specific prevalence of patients with short QT interval in decades according to the number of patients (upper row) and a ratio of patients to the total population of this study (lower row). Histograms of total, male, and female patients are displayed in panels A and D, B and E, and C and F, respectively.

tricular fibrillation (5 repetitive attacks per day) that occurred when bradycardia occurred (Figure 3B). A ventricular pacing lead was emergently introduced into the right ventricle to maintain rapid heart rate. Subsequently, a permanent pacemaker was implanted (DDDR mode, 80 beats/min). Six years after the storm, ventricular fibrillation recurred during a routine pacemaker check. Ventricular fibrillation repeatedly initiated after bradycardia because of threshold margin check. The patient received an implantable cardioverter-defibrillator with atrioventricular sequential pacing applied at a rate of 85 beats/min. Another 54-year-old man developed repetitive syncopal episodes with urinary incontinence in 2001 when sleeping. This patient did not exhibit early repolarization (Figure 4). He did not have a family history of cardiac disorders or sudden unexplained death. This patient revealed no evidence of abnor-

Table 4 ECG characteristics in patients with short and very short QT intervals

	Male			Female		
	Very short (≤355 ms, N = 65)	Short (356 to 362 ms, N = 169)	*P* value	Very short (≤360 ms, N = 36)	Short (361 to 369 ms, N = 157)	*P* value
Heart rate (beats/min)	58.7 ± 8.3	60.3 ± 8.5	.20	60.6 ± 8.5	63.3 ± 9.8	.13
P wave axis (degree)	49.2 ± 37.5	47.8 ± 25.3	.77	47.7 ± 29.4	38.8 ± 28.5	.12
PQ interval (ms)	165.4 ± 37.2	163.4 ± 36.9	.75	161.7 ± 46.6	156.3 ± 39.0	.50
QRS complex duration (ms)	92.6 ± 8.4	92.3 ± 10.0	.82	87.5 ± 7.9	85.9 ± 8.4	.30
R wave axis (degree)	49.3 ± 32.8	57.3 ± 27.1	.060	50.6 ± 31.7	53.4 ± 26.4	.58
QT interval (ms)	357.4 ± 23.7	362.6 ± 22.9	.12	355.4 ± 25.0	360.2 ± 25.8	.31
T wave axis (degree)	46.8 ± 48.5	48.0 ± 34.9	.83	43.2 ± 45.4	48.0 ± 56.7	.64
Atrial fibrillation (N, %)	10, 15.4	13, 7.7	.089	1, 2.8	15, 9.6	.14
Early repolarization (N, %)	3, 4.6	20, 11.8	.076	1, 2.8	2, 1.3	.54

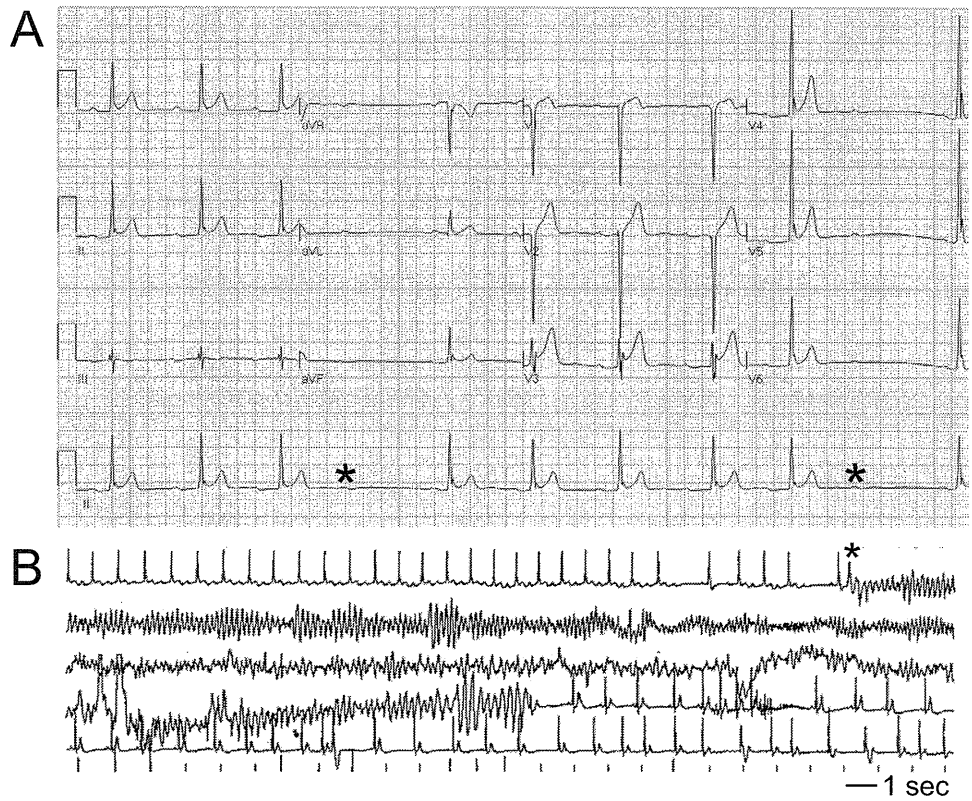

Figure 3 **A:** Twelve-lead ECG of a 22-year-old male patient who developed ventricular fibrillation. Mean heart rate is 50 beats/min; mean QT interval, 364 ms; and mean QTc interval, 332 ms. Early repolarization is present in leads I, II, aVF, and V3-6. *Nonconducting P wave due to Wenckebach atrioventricular block. **B:** Monitored ECG showing occurrence of ventricular fibrillation. *A short-coupled ventricular premature contraction initiated ventricular fibrillation that lasted for >1 minute and then self-terminated.

mality of cardiac function and morphology by transthoracic echocardiography and coronary angiography. His ECG showed Brugada-type ECG after intravenous administration of pilsicainide (Figure 4B). The ST-segment elevation in right precordial leads was accepted as sign of Brugada syndrome in the context of a clinical history, suggesting malignant syncope in this patient. To secure this patient from sudden death, an implantable cardioverter-defibrillator was implanted. These 2 patients did not have gene abnormalities, including *KCNQ1*, *KCNH2*, and *SCN5A*. In addition, we confirmed 6 deceased patients: 2 patients died of pneumonia at 70 and 72 years of age; 1 patient, congestive heart failure at 74 years of age; 1 patient, pancreatic cancer at 70 years of age; 1 patient, colon cancer at 74 years of age; and 1 patient, an unknown cause at 79 years of age. These 6 patients did not have early repolarization. AF was present in 1 patient who died of pneumonia.

Discussion

In the present study, we demonstrated detailed characteristics of patients with short[10–12] QT interval in a large hospital-based population. Consistent with previous reports, patients with short QT interval were rare and had a male preponderance. The age-specific prevalence of patients with short QT interval showed a biphasic distribution with a relatively low prevalence in middle-aged patients. Long-term prognostic assessment revealed that 2 male patients with short QT interval suffered from life-threatening events in this study population.

Characteristics of short QT interval

The present study disclosed distinct characteristics regarding patients with short QT interval. The gender difference in the prevalence of short QT interval that was manifested in this study is presumably due to sex-specific biology, including hormone, membrane ion channel availability, and intracellular signal transduction. A male predominance of patients with short QT interval shown in this study is similar to the fact that QT interval is generally longer in female[13–15] than in male patients. Of interest, the pattern of prevalence of patients with short QT interval exhibited inhomogeneous distribution with 2 peaks at young and old ages in both genders. Although we do not know the mechanism by which this age-dependent distribution had 2 peculiar peaks in patients with short QT interval, one can speculate that the underlying mechanism of short QT interval may be different between young and aged patients because health condition is apparently diverse between them. Further investigations will be needed to explore the mechanism underlying the gender difference and age-specific distribution. Contrary to a previous report,[11] the prevalence of short QT interval in patients with heart rate of <50 beats/min (male, 2.4%;

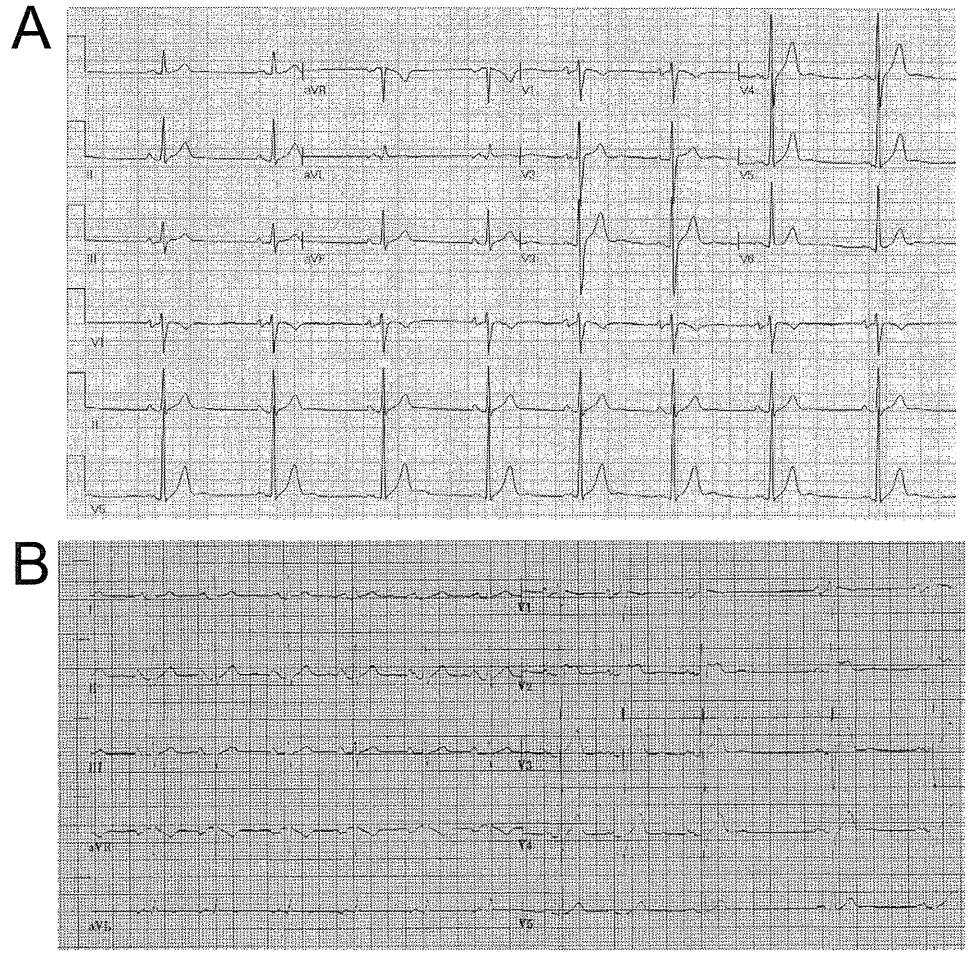

Figure 4 **A:** Twelve-lead ECG of a 54-year-old male patient who developed syncope repeatedly. Mean heart rate is 51 beats/min; mean QT interval, 386 ms; and mean QTc interval, 355 ms. Early repolarization is absent. **B:** ST-segment elevation in right precordial leads by intravenous administration of pilsicainide.

female, 1.6%) was comparable to that in total patients in this study. This is probably due to differential study populations; specifically, the present study population includes only hospital-based patients, and it is therefore possible that many of the patients with slow heart rate were receiving medications that prolonged their QT interval. In contrast, Kobza et al[11] reported on healthy army recruits. We investigated 2 ECG complications of short QT interval: AF and early[4,5,16,17] repolarization. It was reported that AF occurred in patients with short QT syndrome. In this study, the complication rate of AF was much higher compared with the prevalence of AF in the general population of Japan[18] and in total patients in this study (male, 4.1%; female, 1.9%), suggesting atrial involvement of abbreviated action potential with sharing the same mechanism as is present in the ventricle. Early repolarization was usually present in 1% to 5%[19,20] of general populations, which was regarded as benign. The prevalence of early[19,20] repolarization of this study was a little higher than that of those studies and that of the total population of this study (3.9%), but was lower than that of short QT syndrome.[8] To date, Haissaguerre et al[21] reported malignant early repolarization syndrome. In addition, Kamakura et al[22] found that early repolarization was associated with poor outcome in patients with Brugada-type ECG. In these reports, early repolarization was present in inferolateral leads. In contrast, our patient had early repolarization most frequently in anterior leads. Thus, the location of early repolarization may matter in terms of occurrence of life-threatening events.

Short QT interval and short QT syndrome

There may be overlap between the QTc intervals of patients with and without inherited short QT syndrome.[9] The syndrome characterized by extremely abbreviated QT[23,24] interval causes sudden cardiac death. Gene mutation that causes a gain of function in the K^+ channel is attributed to this shortening in this syndrome, suggesting that a specific family[5,16,25] member is affected with this disorder. In general, the QTc interval was <300 ms[4,5,26,27] in subjects with short QT syndrome. In contrast, Antzelevitch et al reported Brugada-type ST-segment elevation in probands whose QT interval was approximately 360 ms. In their cases, gene mutation encoding L-type calcium channel was detected, and those subjects died suddenly. Recently, a mutation of

KCNJ8 was identified in patients with idiopathic ventricular fibrillation and early repolarization, which might be attributed to sudden death.[28] A new mutation in calcium channel regarding congenital short QT syndrome type 6 was reported.[29] A proband of this mutation had a short QT interval of 329 ms; however, a genotype-positive grandmother had a normal QT interval of 432 ms, although she had myocardial infarction. This study suggests that a phenotypical QT interval might be modified by myocardial necrosis in this syndrome, giving rise to normalization. Thus, one has to consider lack of genotype-phenotype correlation in short QT syndrome. However, genetic mutation was not detected in 2 patients who experienced life-threatening events in this study. Therefore, further investigations of gene analysis are needed in these patients.

Arrhythmogenesis in short QT interval

Gallagher et al[12] reported that a QTc interval of ≤330 ms was extremely rare in healthy subjects and did not bear a significant risk of sudden death. However, in our hospital-based population, 2 patients with short QTc interval developed life-threatening events. An experimental study that dealt with an association of early repolarization with ventricular fibrillation showed that modulating factors amplified transmural electrical heterogeneity that caused early repolarization to generate reentry.[26] In this study, 1 patient who experienced bradycardia-dependent occurrence of ventricular fibrillation presented J wave. This finding suggests manifestation of transmural electrical gradient during slow heart rate,[30–32] which is consistent with previous reports. Another patient who exhibited Brugada-type ECG after the administration of sodium channel blocker suggests that a mechanism underlying life-threatening events in short QT syndrome may be similar to a mechanism accounting for ventricular fibrillation in Brugada syndrome. In clinical practice, it is difficult to diagnose short QT syndrome unless a subject is symptomatic. Indeed, 2 patients who had developed life-threatening events in this study were found to have a short QT interval afterward. This finding indicates incidental discovery of short QT syndrome.

Study limitations

First, patients enrolled in this study were derived from a hospital-based population, indicating that our data do not properly apply to a general population. Because our data were based on the hospital population, patients who had organic heart diseases or took drugs with QT-prolonging effects were involved. We could not search medication uses thoroughly, as Ramirez et al[33] did. In addition, patients with bundle branch block or pre-excitation syndrome were not excluded from the analysis. The QT interval was longer when computer-assisted measure was performed as compared with manual measure of QT interval in lead V5. These underlie the right-skewed distributions of QTc interval. The fact that we included patients with medications probably had a limited effect on the number of patients with very short QT because medications (and conditions such as bundle branch block) tend to prolong the QT, not to shorten it. Second, we could assess the prognosis of 327 patients (77%) with short QT interval. However, the long-term outcome was not thoroughly investigated and the follow-up period was not long enough. Further assessment is necessary to clarify the prognosis of patients with short QT interval. Third, it must be considered how to correct QT interval. Correlation of QT interval by the Bazett formula has a tendency to overestimate or underestimate QT interval when heart rate is particularly fast or slow, respectively. We first set the heart rate to ranging from 50 to 100 beats/min not to include overestimation and underestimation of QT interval by the Bazett formula. Even in an additional analysis in patients with heart rate <50 beats/min, the prevalence of short QT interval was similar to that in the first analysis. This might be attributed to our hospital-based population.

Conclusion

Until now, there have been mounting reports of short QT syndrome. Nevertheless, ECG features of prognostic significance are still lacking. This study proposed that early repolarization concomitant with short QT interval indicates a potential for sudden cardiac death. The complication rate of AF and early repolarization was higher in patients with short QT interval than in a general population and total patients of this study. Although our database contains a huge number of ECGs, we could assess a rather small group of patients with short QT interval. This implies that multicenter clinical research will be required to further determine the prognostic value of short QT interval. Despite the small number of patients enrolled in this study, the findings could shed light on the prognostic value of early repolarization in patients with short QT interval.

Acknowledgements

The authors thank Kahaku Emoto, Seiichi Fujisaki, and Tatsumi Uchiyama (GE Yokokawa Medical System Co.) for their technical assistance.

Appendix

Supplementary data

Supplementary data associated with this article can be found, in the online version, at doi:10.1016/j.hrthm.2011.08.016.

References

1. Montanez A, Ruskin JN, Hebert PR, Lamas GA, Hennekens CH. Prolonged QTc interval and risks of total and cardiovascular mortality and sudden death in the general population: a review and qualitative overview of the prospective cohort studies. Arch Intern Med 2004;164:943–948.
2. Robbins J, Nelson JC, Rautaharju PM, Gottdiener JS. The association between the length of the QT interval and mortality in the Cardiovascular Health Study. Am J Med 2003;115:689–694.
3. Roden DM. Keep the QT interval: it is a reliable predictor of ventricular arrhythmias. Heart Rhythm 2008;5:1213–1215.
4. Gaita F, Giustetto C, Bianchi F, et al. Short QT syndrome: a familial cause of sudden death. Circulation 2003;108:965–970.
5. Bellocq C, van Ginneken AC, Bezzina CR, et al. Mutation in the KCNQ1 gene leading to the short QT-interval syndrome. Circulation 2004;109:2394–2397.

6. Priori SG, Pandit SV, Rivolta I, et al. A novel form of short QT syndrome (SQT3) is caused by a mutation in the KCNJ2 gene. Circ Res 2005;96:800–807.
7. Morita H, Wu J, Zipes DP. The QT syndromes: long and short. Lancet 2008; 372:750–763.
8. Watanabe H, Makiyama T, Koyama T, et al. High prevalence of early repolarization in short QT syndrome. Heart Rhythm 2010;7:647–652.
9. Viskin S. The QT interval: too long, too short or just right. Heart Rhythm 2009;6:711–715.
10. Anttonen O, Junttila MJ, Rissanen H, Reunanen A, Viitasalo M, Huikuri HV. Prevalence and prognostic significance of short QT interval in a middle-aged Finnish population. Circulation 2007;116:714–720.
11. Kobza R, Roos M, Niggli B, et al. Prevalence of long and short QT in a young population of 41,767 predominantly male Swiss conscripts. Heart Rhythm 2009; 6:652–657.
12. Gallagher MM, Magliano G, Yap YG, et al. Distribution and prognostic significance of QT intervals in the lowest half centile in 12,012 apparently healthy persons. Am J Cardiol 2006;98:933–935.
13. Makkar RR, Fromm BS, Steinman RT, Meissner MD, Lehmann MH. Female gender as a risk factor for torsades de pointes associated with cardiovascular drugs. JAMA 1993;270:2590–2597.
14. Pham TV, Rosen MR. Sex, hormones, and repolarization. Cardiovasc Res 2002;53:740–751.
15. James AF, Choisy SC, Hancox JC. Recent advances in understanding sex differences in cardiac repolarization. Prog Biophys Mol Biol 2007;94:265–319.
16. Brugada R, Hong K, Dumaine R, et al. Sudden death associated with short-QT syndrome linked to mutations in HERG. Circulation 2004;109:30–35.
17. Hong K, Bjerregaard P, Gussak I, Brugada R. Short QT syndrome and atrial fibrillation caused by mutation in KCNH2. J Cardiovasc Electrophysiol 2005; 16:394–396.
18. Inoue H, Fujiki A, Origasa H, et al. Prevalence of atrial fibrillation in the general population of Japan: an analysis based on periodic health examination. Int J Cardiol 2009;137:102–107.
19. Klatsky AL, Oehm R, Cooper RA, Udaltsova N, Armstrong MA. The early repolarization normal variant electrocardiogram: correlates and consequences. Am J Med 2003;115:171–177.
20. Wellens HJ. Early repolarization revisited. N Engl J Med 2008;358:2063–2065.
21. Haissaguerre M, Derval N, Sacher F, et al. Sudden cardiac arrest associated with early repolarization. N Engl J Med 2008;358:2016–2023.
22. Kamakura S, Ohe T, Nakazawa K, et al. Long-term prognosis of probands with Brugada-pattern ST-elevation in leads V1-V3. Circ Arrhythm Electrophysiol 2009;2:495–503.
23. Schimpf R, Wolpert C, Gaita F, Giustetto C, Borggrefe M. Short QT syndrome. Cardiovasc Res 2005;67:357–366.
24. Giustetto C, Di Monte F, Wolpert C, et al. Short QT syndrome: clinical findings and diagnostic-therapeutic implications. Eur Heart J 2006;27:2440–2447.
25. Itoh H, Sakaguchi T, Ashihara T, et al. A novel KCNH2 mutation as a modifier for short QT interval. Int J Cardiol 2009;137:83–85.
26. Gussak I, Antzelevitch C. Early repolarization syndrome: clinical characteristics and possible cellular and ionic mechanisms. J Electrocardiol 2000;33:299–309.
27. Antzelevitch C, Pollevick GD, Cordeiro JM, et al. Loss-of-function mutations in the cardiac calcium channel underlie a new clinical entity characterized by ST-segment elevation, short QT intervals, and sudden cardiac death. Circulation 2007;115:442–449.
28. Haissaguerre M, Chatel S, Sacher F, et al. Ventricular fibrillation with prominent early repolarization associated with a rare variant of KCNJ8/KATP channel. J Cardiovasc Electrophysiol 2009;20:93–98.
29. Templin C, Ghadri JR, Rougier JS, et al. Identification of a novel loss-of-function calcium channel gene mutation in short QT syndrome (SQTS6). Eur Heart J 2011;32:1077–1088.
30. Aizawa Y, Tamura M, Chinushi M, et al. Idiopathic ventricular fibrillation and bradycardia-dependent intraventricular block. Am Heart J 1993;126:1473–1474.
31. Kalla H, Yan GX, Marinchak R. Ventricular fibrillation in a patient with prominent J (Osborn) waves and ST segment elevation in the inferior electrocardiographic leads: a Brugada syndrome variant? J Cardiovasc Electrophysiol 2000;11:95–98.
32. Takagi M, Aihara N, Takaki H, et al. Clinical characteristics of patients with spontaneous or inducible ventricular fibrillation without apparent heart disease presenting with J wave and ST segment elevation in inferior leads. J Cardiovasc Electrophysiol 2000;11:844–848.
33. Ramirez AH, Schildcrout JS, Blakemore DL, et al. Modulators of normal electrocardiographic intervals identified in a large electronic medical record. Heart Rhythm 2011;8:271–277.

Circulation Journal
Official Journal of the Japanese Circulation Society
http://www.j-circ.or.jp

ORIGINAL ARTICLE
Arrhythmia/Electrophysiology

KCNE3 T4A as the Genetic Basis of Brugada-Pattern Electrocardiogram

Tadashi Nakajima, MD, PhD; Jie Wu, PhD; Yoshiaki Kaneko, MD, PhD; Takashi Ashihara, MD, PhD; Seiko Ohno, MD, PhD; Tadanobu Irie, MD; Wei-Guang Ding, MD, PhD; Hiroshi Matsuura, MD, PhD; Masahiko Kurabayashi, MD, PhD; Minoru Horie, MD, PhD

Background: Brugada syndrome (BrS) is genetically heterogeneous. In Japanese BrS patients, except for *SCN5A* and *KCNE5*, mutations in the responsible genes have not yet been identified, and therefore the genetic heterogeneity remains poorly elucidated.

Methods and Results: Forty consecutive patients with Brugada-pattern electrocardiogram (ECG) underwent comprehensive genetic analysis of BrS-causing genes including *SCN5A*, *SCN1B*, *SCN3B*, *CACNA1C*, *CACNB2*, *KCNE3* and *KCNE5*. Besides identifying 8 *SCN5A* mutations in the present cohort, a *KCNE3* T4A mutation was found in a 55-year-old male patient who had experienced several episodes of syncope. A head-up tilt test during passive tilt provoked both hypotension and bradycardia, followed by syncope. He was therefore diagnosed with neurally mediated syncope (NMS). To characterize the functional consequence of the mutant, electrophysiological experiments using whole-cell patch-clamp methods and computer simulations using human right ventricular wall model were carried out. It was found that KCNE3 T4A increased I_{to} recapitulated by heterologously coexpressing Kv4.3+KChIP2b+KCNE3-wild type or KCNE3-T4A in CHO cells.

Conclusions: A *KCNE3* T4A mutation was identified in a Japanese patient presenting Brugada-pattern ECG and NMS. Its functional consequence was the gain of function of I_{to}, which could underlie the pathogenesis of Brugada-pattern ECG. The data provide novel insights into the genetic basis of Japanese BrS. (*Circ J* 2012; **76:** 2763–2772)

Key Words: Brugada syndrome; I_{to}; *KCNE3*; Mutation; Neurally mediated syncope

Brugada syndrome (BrS) is a hereditable disorder characterized by ST-segment elevations in the right precordial electrocardiogram (ECG) leads, associated with a high incidence of syncope or sudden death due to ventricular tachyarrhythmias, which mostly affects men. BrS is genetically heterogeneous, and has been linked to mutations in genes that perturb cardiac ion currents (I_{Na}, I_{Ca}, $I_{K\text{-}ATP}$ and I_{to}) contributing to the early phase of action potential (AP).[1–12] Among the BrS-causing genes, mutations in *SCN5A* (encoding the pore-forming α-subunit of the cardiac voltage-gated sodium channel) have accounted for the major form of BrS in approximately 20% of cases, and other gene mutations for approximately 10%,[1,2] thus around 70% of BrS cases remain to be genetically elucidated.

The transient outward potassium current (I_{to}) in the heart functions mainly during the early phase of AP because it activates and inactivates rapidly on membrane depolarization. Predominant expression of I_{to} in ventricular epimyocardium compared to endomyocardium, especially in the right ventricle, contributes to the rapid repolarization and the initial plateau formation of the AP (AP notch).[13–15] Experimental studies suggested that the gain of function of I_{to} leads to augmentation of the AP notch in epimyocardium but not in endomyocardium, thus resulting in the enhancement of transmural voltage gradient during the ventricular repolarization, which is thought to be responsible for the ST-segment elevation in the right pre-

Received April 25, 2012; revised manuscript received July 26, 2012; accepted August 7, 2012; released online September 13, 2012 Time for primary review: 28 days

Department of Medicine and Biological Science, Gunma University Graduate School of Medicine, Maebashi (T.N., Y.K., T.I., M.K.); Department of Cardiovascular and Respiratory Medicine (J.W., T.A., S.O., M.H.), Department of Physiology (W.-G.D., H.M.), Shiga University of Medical Science, Otsu, Japan; and Department of Pharmacology, Medical School of Xi'an Jiaotong University, Xi'an, Shaanxi (J.W.), China

The first two authors contributed equally to this work (T.N., J.W.).

Mailing address: Minoru Horie, MD, PhD, Department of Cardiovascular and Respiratory Medicine, Shiga University of Medical Science, Seta Tsukinowa-cho, Otsu 520-2192, Japan. E-mail: horie@belle.shiga-med.ac.jp

ISSN-1346-9843 doi:10.1253/circj.CJ-12-0551

cordial ECG leads (Brugada-pattern ECG) in BrS.[14] Further augmentation of the AP notch in epimyocardium causes the loss of AP plateau phase (dome), which consequently leads to arrhythmogenesis in BrS defined as phase 2 reentry.[14] I_{to} in human ventricle is thought to be consist of α-subunit Kv4.3 (encoded by *KCND3*) and β-subunits including Kv channel interacting protein (KChIP), KCNE, diaminopeptidyl transferase-like protein (DPP) and Kvβ families.[16–24] Accordingly, mutations in the related genes that increase I_{to} may underlie the pathogenesis of BrS.

KCNE3, 1 member of the *KCNE* gene family (*KCNE1–5*), modulates the function of Kv4.3 as an inhibitory β-subunit.[19,20] Recently, Delpón et al identified a *KCNE3* R99H mutation in 1 BrS family.[6] Functional analysis using the heterologous expression system that recapitulates I_{to} by coexpression of Kv4.3 with KCNE3-wild type (WT)/R99H showed that KCNE3 R99H causes a gain of function of I_{to} by a dominant-positive effect, thus precipitating the development of BrS.[6] Moreover, mutations in Kv4.3 and *KCNE5*, which also functions as an inhibitory β-subunit of I_{to}, were identified in BrS patients.[9,10] Functional analysis of these mutations showed that they increase I_{to}.[9,10] Therefore, it was established that the gain of function of I_{to} by mutations in genes that encode I_{to} could be one of the causes of BrS.

We have previously reported the identification of 8 mutations in *SCN5A* among 30 consecutive Japanese patients with Brugada-pattern ECG.[25] Considering that the genetic heterogeneity of BrS is poorly elucidated in Japan,[10,26,27] we further conducted genetic screening of BrS-causing genes among the 30 consecutive patients and another 10 new patients with Brugada-pattern ECG, and identified a *KCNE3* T4A mutation in a patient presenting with neurally mediated syncope (NMS). In the present study, we describe the clinical phenotype of the *KCNE3* T4A carrier, and characterize the functional consequence of the I_{to} recapitulated by heterologously coexpressing Kv4.3 + KChIP2b + KCNE3-T4A in CHO cells. Furthermore, we performed computer simulations based on the I_{to} obtained in electrophysiological recordings, and showed that KCNE3-T4A recapitulated the ECG phenotype.

Methods

Subjects

The present subjects were 40 consecutive patients (probands; 35 male, 47±16 years of age) with Brugada-pattern ECG who were referred to Gunma University Hospital between April 2002 and September 2010. All patients, except for patient 27, presented with coved-type ST-elevation in the right precordial ECG leads with or without provocation of Na channel blocker (pilsicainide: 1 mg/kg, or procainamide 5 mg/kg), although it is still under debate whether patients with drug-induced Brugada-pattern ECG have poor prognosis.[28,29] Echocardiography and conventional left catheterization, if performed, indicated no structural heart disease in all the patients. Thirty-two patients underwent electrophysiological assessment. Up to 3 extra stimuli (minimum coupling interval: 180 ms) were delivered from 2 ventricular sites (right ventricular apex and right ventricular outflow tract). A head-up tilt (HUT) test was performed using the same protocol as described previously.[30] Clinical features of the subjects are listed in Table 1.

Genetic Analysis

After obtaining appropriate approval from the institution review board and written informed consent from the patient, genomic DNA was extracted from peripheral blood lymphocytes using the standard protocol of the QIAamp DNA Blood Midi Kit (QIAGEN, Hilden, Germany). All coding exons of *SCN5A*, *SCN1B*, *KCNE3*, *SCN3B* and *KCNE5*, and their splice sites were amplified on polymerase chain reaction (PCR) using primers flanking the intronic sequences as reported previously.[1,5–7,25,31] The PCR products were purified and directly sequenced using an ABI PRISM 3130 Genetic Analyzer (Applied Biosystems, Foster City, CA, USA). Regarding patient 18, *CACNA1C* and *CACNB2* were also analyzed.[4] The mutation was analyzed twice on independent PCR amplification and sequencing. *KCNE3* T4A was not identified in 528 control alleles.

Heterologous Expression of hKv4.3 and β-Subunits in CHO Cells

Full-length cDNA fragment of WT KCNE3 in pCR3.1 vector was subcloned into pIRES-CD8 vector that is useful in cell selection. The KCNE3 mutant (T4A) was constructed using a Quick Change II XL site-directed mutagenesis kit according to the manufacturer's instructions (Stratagene, La Jolla, CA, USA) and subcloned to the same vector. The KCNE3 mutant was fully sequenced (ABI PRISM 3130 Genetic analyzer) to ensure fidelity. Full-length cDNA encoding the short isoform of human Kv4.3 (hKv4.3) subcloned into the pIRES-GFP (Clontech, Palo Alto, CA, USA) expression vector was kindly provided by Dr GF Tomaselli (Johns Hopkins University). Full-length cDNA encoding Kv channel-interacting protein 2b (KChIP2b) subcloned into the PCMV-IRS expression vector was a kind gift from Dr GN Tseng (Virginia Commonwealth University). Kv4.3 was transiently transfected into CHO cells together with KChIP2b and KCNE3-WT (or T4A) cDNA at equimolar ratio (Kv4.3, 1.0 μg; KChIP2b, 1.0 μg; KCNE3, 1.0 μg) using Lipofectamine (Invitrogen Life Technologies, Carlsbad, CA, USA) according to the manufacturer's instructions. In a subset of experiments, 0.5 μg KCNE3-WT and 0.5 μg KCNE3-T4A were co-transfected into cells with 1.0 μg Kv4.3 and 1.0 μg KChIP2b. The transfected cells were then cultured in Ham's F-12 medium (Nakalai Tesque, Kyoto, Japan) as described previously.[24]

Electrophysiologic Recording and Data Analysis

After 48 h of transfection, a coverslip with cells was transferred to a 0.5-ml bath chamber at 25°C on an inverted microscope stage and perfused at 1–2 ml/min with extracellular solution containing the following (in mmol/L): 140 NaCl, 5.4 KCl, 1.8 $CaCl_2$, 0.5 $MgCl_2$, 0.33 NaH_2PO_4, 5.5 glucose, and 5.0 HEPES; pH 7.4 with NaOH. Cells that emitted green fluorescence were chosen for patch-clamp experiments. If coexpressed with KCNE3 (or its mutant), the cells were incubated with polystyrene microbeads precoated with anti-CD8 antibody (Dynabeads M450, Dynal, Norway) for 15 min. In these cases, cells that emitted green fluorescence and had attached beads were chosen for electrophysiologic recording. Whole-cell membrane currents were recorded with an EPC-8 patch-clamp amplifier (HEKA, Lambrecht, Germany), and data were low-pass filtered at 1 kHz, acquired at 5 kHz through an LIH-1600 analog-to-digital converter (HEKA), and stored on hard disk using PulseFit software (HEKA). Patch pipettes had a resistance of 2.5–5.0 mol/LΩ when filled with the following pipette solution (in mmol/L): 70.0 potassium aspartate, 50.0 KCl, 10.0 KH_2PO_4, 1.0 $MgSO_4$, 3.0 Na_2-ATP (Sigma, Japan, Tokyo), 0.1 Li_2-GTP (Roche Diagnostics, Mannheim, Germany), 5.0 EGTA, and 5.0 HEPES (pH 7.2).

Whole cell currents were elicited in a series of depolarizing voltage steps from a holding potential of –80 mV. The time

Table 1. Clinical Features and Genetic Analysis in Brugada-Pattern ECG Patients

Patient no.	Sex	Age (years)	ECG	Symptom	FH	EPS	ICD	*SCN5A*	*SCN1B*	*SCN3B*	*KCNE3*	*KCNE5*
1	M	49	Coved (P)	Sy	No	VF	Yes	c.393–1 c>t**				
2	F	58	Coved	Asy	No	N/A	No	R1193Q				
3	M	36	Coved (P)	Asy	No	VF	No	A586T**				
4	M	29	Coved (P)	Sy	No	VF	Yes		L210P, S248R, R250T			
5	M	56	Coved	CPA	No	VF	Yes		L210P			
6	M	30	Coved	CPA	No	VF	Yes					
7	M	42	Coved (P)	Sy	No	No VF	Yes					
8	M	53	Coved (P)	CPA	No	No VF	Yes		R187H, L210P			
9	M	45	Coved	CPA	No	VF	Yes	P1090L	L210P, S248R, R250T			
10	M	47	Coved (P)	CPA	No	VF	Yes		L210P			
11	M	39	Coved (P)	Asy	No	NSVT	No		L210P			
12	M	32	Coved	Asy	Yes	N/A	Yes		L210P, S248R, R250T			
13	M	42	Coved (Pro)	Sy	No	VF	Yes	P1090L, R1232W				
14	M	59	Coved (P)	Asy	No	No VF	No	c.4437+5 g>a				
15	M	64	Coved	Asy	No	N/A	No		L210P*, S248R*, R250T*			
16	M	39	Coved (P)	Asy	No	NSVT	No					
17	M	61	Coved (P)	Asy	Yes	NSVT	No	R689H**				
18	M	55	Coved (P)	Sy	No	NSVT	No				T4A**	
19	M	37	Coved (P)	Sy	Yes	VF	Yes		L210P, S248R, R250T			
20	M	49	Coved (P)	Asy	No	No VF	No	H558R*, S1553R**				
21	F	38	Coved (P)	Asy	No	N/A	No					
22	M	64	Coved (P)	Asy	Yes	VF	Yes	H558R, R1193Q	L210P, S248R, R250T			
23	M	71	Coved (P)	CPA	No	No VF	Yes	P1090L	L210P*, S248R*, R250T*			
24	M	44	Coved (P)	Sy	Yes	VF	Yes	E1784K**				
25	M	56	Coved (P)	Sy	No	VF	Yes		L210P, S248R, R250T			
26	M	15	Coved	Sy	No	N/A	No		L210P*, S248R, R250T			
27	M	25	Saddle-back	Sy	Yes	No VF	Yes	V1951M**				
28	F	67	Coved (P)	Asy	No	N/A	No					
29	F	28	Coved	Asy	No	N/A	No	Q1706H**				
30	M	38	Coved	Sy	No	NSVT	No					
31	M	30	Coved (P)	Asy	No	No VF	No					
32	M	63	Coved (P)	Asy	No	NSVT	No		L210P, S248R, R250T			
33	M	43	Coved	Asy	No	VF	No					
34	M	57	Coved	Asy	No	No VF	No		L210P, S248R, R250T			
35	M	40	Coved (P)	Sy	No	VF	Yes		L210P, S248R, R250T			
36	M	66	Coved (P)	Sy	No	VF	Yes		L210P			
37	M	72	Coved (P)	Asy	No	VF	No		L210P, S248R, R250T			
38	M	33	Coved	Asy	No	NSVT	No					
39	M	77	Coved	Asy	No	VF	No		L210P, S248R, R250T			
40	F	15	Coved (P)	CPA	No	N/A	Yes	A735E**				

Mutations and non-synonymous variants are listed. *Homozygous; **mutations.
Asy, asymptomatic; CPA, cardiopulmonary arrest; ECG, electrocardiogram; EPS, up to 3 extrastimuli from right ventricular apex and right ventricular outflow tract; FH, family history of sudden death under age 45; N/A, not accessed; NSVT, non-sustained ventricular tachycardia; P, pilsicainide provocation; Pro, procainamide provocation; Sy, syncope; VF, ventricular fibrillation.

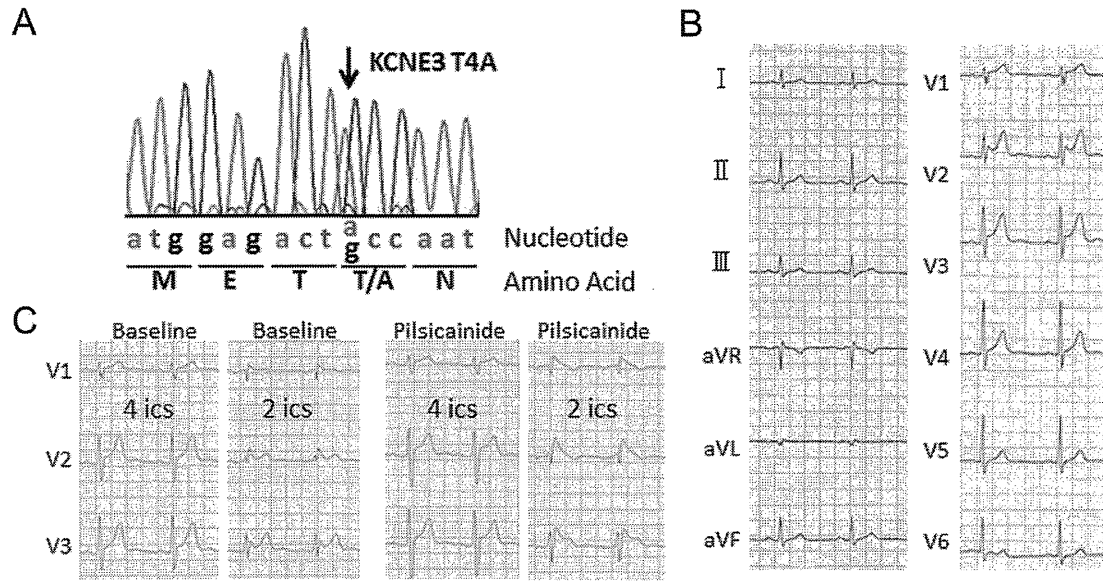

Figure 1. (A) Direct sequencing of the *KCNE3* gene in the index patient. Nucleotide and amino acid substitutions are indicated below. (B) Twelve-lead ECG recorded 2 months before admission. (C) V_{1-3} lead electrocardiogram before (baseline) and after pilsicainide provocation (Pilsicainide). ics, intercostal space.

interval between each voltage pulse was 10 s. The difference between the peak current amplitude and the current at the end of a test pulse was referred to as the transient outward current. To control for cell size variability, currents are expressed as densities (pA/pF) as described previously.[24] Steady-state activation curves were obtained by plotting the normalized conductance as a function of peak outward potentials. Steady-state inactivation curves were generated by a standard 2-pulse protocol with a conditioning pulse of 500 ms and obtained by plotting the normalized current as a function of the test potential. Steady-state inactivation/activation kinetics were fitted to the following Boltzmann equation:

$$Y(V)=1/(1+\exp[(V_{1/2}-V)/k]),$$

where Y = normalized conductance or current, $V_{1/2}$ = potential for half-maximum inactivation or activation, respectively, and k = slope factor.

Data relative to inactivation time constants, time to peak, and mean current levels were obtained using current data recorded at +50 mV. Recovery from inactivation was assessed using a standard paired-pulse protocol: a 1-s test pulse to +50 mV (P1) followed by a variable recovery interval at –80 mV and then a second test pulse to +50 mV (P2). Both the inactivation time constants and the time constant for recovery from inactivation were determined by fitting the data to a single exponential:

$$I(t)\ (\text{or } P2/P1)=A+B\exp(-t/\tau),$$

where I(t) = current amplitude at time t, A and B = constants, and τ = inactivation time constant or time constant for recovery from inactivation. For measurement of recovery from inactivation, the plot of P2/P1 instead of I(t) was used.

All data are given as mean±SEM. Statistical comparisons between 2 groups were analyzed using Student's unpaired t-test. Comparisons among multiple groups were analyzed using analysis of variance followed by Dunnett test. $P<0.05$ was considered significant.

Computer Simulation

To confirm the exact role of the *KCNE3* T4A mutation, we conducted simulations of paced propagation in a 0.5-cm 1-D bidomain myocardial model with transverse conductivity, mimicking transmural section of right ventricular wall. Membrane kinetics were represented by the Priebe-Beuckelmann human ventricular model,[32] of which original I_{to} was replaced by the I_{to} with KCNE3-WT or KCNE3-T4A mutation obtained in electrophysiologic recording.

To obtain the transmural gradient in the right ventricular wall, we defined endocardial and epicardial tissues as each of length 0.25 cm, and we set the conductances of the slowly activating component of the delayed rectifier potassium channel (I_{Ks}), the inward rectifier potassium channel (I_{K1}), and I_{to} in the endocardial layers to 46%, 82%, and 29%, respectively, of those in the epicardial layers. Pacing stimuli of 2 ms and strength twice-diastolic threshold were applied transmembranously to the endocardial end at a cycle length of 1,000 ms. The time and spatial discretization steps were 10 μs and 50 μm, respectively. Other model parameters and the numerical approach have been described elsewhere.[33]

Results

Genetic Analysis

We conducted comprehensive genetic analysis of BrS-causing genes including *SCN5A*, *SCN1B*, *KCNE3*, *SCN3B* and *KCNE5*, among 40 consecutive patients with Brugada-pattern ECG. Besides identifying 8 *SCN5A* mutations in the present cohort, we also found a T4A mutation in *KCNE3* in the patient 18 who had no mutations in the other genes (including *CACNA1C* and *CACNB2*) associated with BrS (**Figure 1A**; **Table 1**).

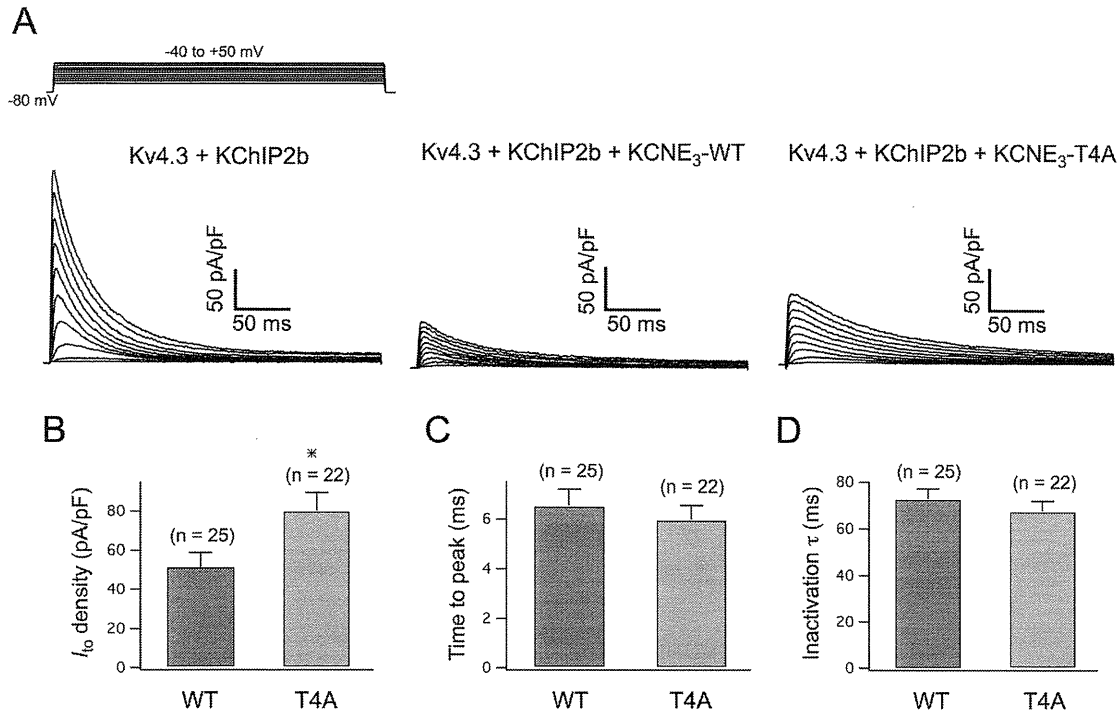

Figure 2. KCNE3-T4A increased I_{to} current reconstituted by coexpression of 1 μg Kv4.3 + 1 μg KChIP2b + 1 μg KCNE3 in CHO cells. (**A**) Representative current traces recorded from cells expressing (**Left**) Kv4.3 + KChIP2b, (**Middle**) Kv4.3 + KChIP2b + KCNE3-WT and (**Right**) Kv4.3 + KChIP2b + KCNE3-T4A. **Inset**, depolarizing test pulses introduced from –80 mV holding potential to potentials ranging from –40 to +50 mV, with 300-ms duration, in 10-mV increments. (**B**) Peak current density of I_{to}, (**C**) time to peak of activation course and (**D**) inactivation time constants recorded at +50 mV. (n), no. of experiments. *P<0.05 vs. WT.

Clinical Presentation

A 55-year-old man (patient 18) was referred to hospital to examine the cause of syncope. He had experienced several episodes of syncope under specific conditions, such as when sitting at a funeral, and standing up after drinking alcohol, since his 30 s. He had no previous history of illness except for syncopal episodes, and no family history of sudden cardiac death. A physical examination, chest X-ray, and blood test showed no remarkable abnormalities. His 12-lead ECG, recorded 2 months before admission, showed saddle-back-type ST-segment elevation in the right precordial ECG leads (**Figure 1B**). The QTc interval was 414 ms. A coved-type ST-segment elevation in the right precordial ECG leads at the second intercostal space appeared after provocation with pilsicainide (**Figure 1C**). Signal-averaged ECG showed no late potentials. Transthoracic echocardiography showed no apparent structural heart disease.

The patient underwent electrophysiological assessment. Up to 3 extrastimuli induced non-sustained polymorphic ventricular tachycardia, but not ventricular fibrillation. An HUT test was performed because syncopal episodes had occurred under specific conditions that could evoke NMS. The HUT test during passive tilt provoked both hypotension and bradycardia, followed by syncope. Therefore, the patient was diagnosed as having NMS. The patient was not prescribed medication or implanted with an implantable cardioverter defibrillator.

KCNE3-T4A Mutation Increased the Current Amplitude of the Kv4.3 + KChIP2b + KCNE3 Channel

Because KCNE3 was shown to co-associate with Kv4.3 in the human heart, and I_{to} is thought to underlie the development of Brugada phenotype,[6,15] KCNE3-WT/T4A was coexpressed together with Kv4.3 and KChIP2b, which has been shown to serve as a principal β-subunit of I_{to}.[18,19,34,35] **Figure 2A** shows representative whole-cell current traces recorded from CHO cells expressing Kv4.3 + KChIP2b, Kv4.3 + KChIP2b + KCNE3-WT and Kv4.3 + KChIP2b + KCNE3-T4A.

Consistent with the previous literature, coexpression of KCNE3-WT dramatically reduced the current amplitude of the Kv4.3 + KChIP2b channel.[6,20,24] Further analysis of peak current showed that the current density of the coexpression with the KCNE3-T4A mutant was significantly larger than that for KCNE3-WT (Kv4.3 + KChIP2b + KCNE3-WT, 51.7±7.3 pA/pF, n=25 vs. Kv4.3 + KChIP2b + KCNE3-T4A, 80.2±9.1 pA/pF, n=22, P<0.05; **Figure 2A,B**). **Figure 2C** shows mean time interval from the onset of the pulse to maximum current (time to peak), and **Figure 2D** shows the time constants (τ) of inactivation obtained using a single exponential at +50 mV. These data indicate that KCNE3-T4A mutation increased the current amplitude of the Kv4.3 + KChIP2b + KCNE3 channel, but did not affect time to peak and the inactivation time course.

Effect of KCNE3-T4A on Activation/inactivation Kinetics of Kv4.3 + KChIP2b + KCNE3 Channels

To further examine the effect of KCNE3-T4A on gating kinet-

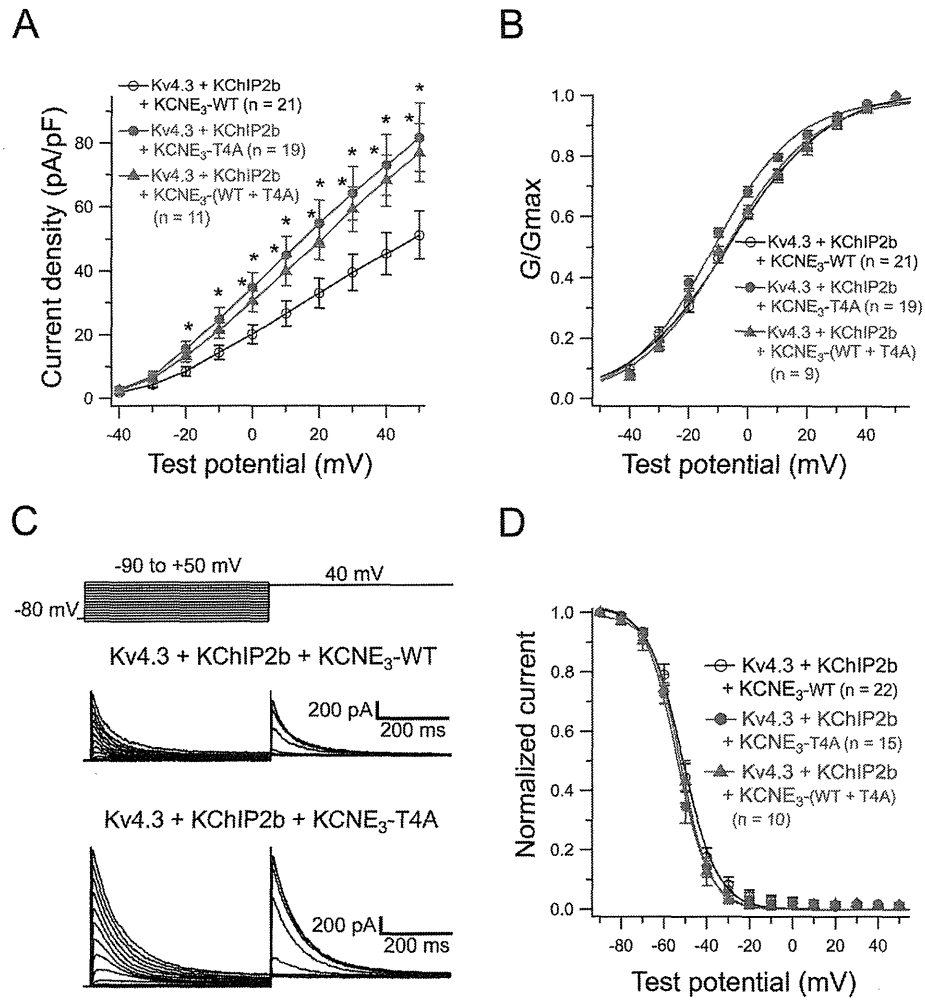

Figure 3. Effect of KCNE3-T4A on activation/inactivation kinetics of Kv4.3+KChIP2b+KCNE3 channels. (**A**) Current–voltage relationship curves showing peak current densities of the (open circles) Kv4.3+KChIP2b+KCNE3-WT, (closed circles) KCNE3-T4A and (filled triangles) KCNE3-(0.5μg WT+0.5μg T4A) channels. *P<0.05 vs. Kv4.3+KChIP2b+KCNE3-WT. (**B**) Normalized conductance-voltage relationships for peak currents in (**A**). (**C**) (**Upper**) Representative Kv4.3+KChIP2b+KCNE3-WT, (**Lower**) Kv4.3+KChIP2b+KCNE3-T4A current traces induced by 500-ms pre-pulses from –90mV to +50mV applied from the holding potential –80mV in 10-mV steps followed by a second pulse to +40mV (fixed) for assessing the inactivation process. (**D**) Steady-state inactivation curves for the (open circles) Kv4.3+KChIP2b+KCNE3-WT, (closed circles) KCNE3-T4A, and (filled triangles) KCNE3-(WT+T4A) channels. Peak currents thus measured were normalized by that obtained from the –90mV pre-pulse and are plotted against the pre-pulse potentials. Smooth curves were drawn by fitting to the Boltzmann equation.

Table 2. Current Density and Biophysical Kinetics

	Current density	Activation	Steady-state activation		Steady-state inactivation		Inactivation	Recovery from inactivation
	At+50mV (pA/pF)	Time to peak (ms)	$V_{1/2}$ (mV)	k (mV)	$V_{1/2}$ (mV)	k (mV)	τ (ms)	τ (ms)
Kv4.3+KChIP2b+KCNE3-WT	51.7±7.3 (n=25)	6.6±0.7 (n=25)	–6.5±2.0 (n=21)	17.2±1.1 (n=21)	–52.7±1.7 (n=22)	–9.9±1.7 (n=22)	73.0±4.2 (n=25)	65.7±10.2 (n=9)
Kv4.3+KChIP2b+KCNE3-T4A	80.2±9.1† (n=22)	6.0±0.6 (n=22)	–11.6±1.2† (n=19)	14.2±0.8 (n=19)	–54.7±1.6 (n=15)	–8.8±2.1 (n=15)	67.1±4.1 (n=22)	66.9±10.7 (n=9)
Kv4.3+KChIP2b+KCNE3-(WT+T4A)	77.7±8.6† (n=11)	6.7±0.8 (n=11)	–7.2±1.1 (n=10)	15.4±0.8 (n=10)	–52.2±2.0 (n=10)	–6.1±1.1 (n=10)	64.3±9.8 (n=11)	72.8±12.6 (n=6)

†P<0.05 vs. Kv4.3+KChIP2b+KCNE3-WT.

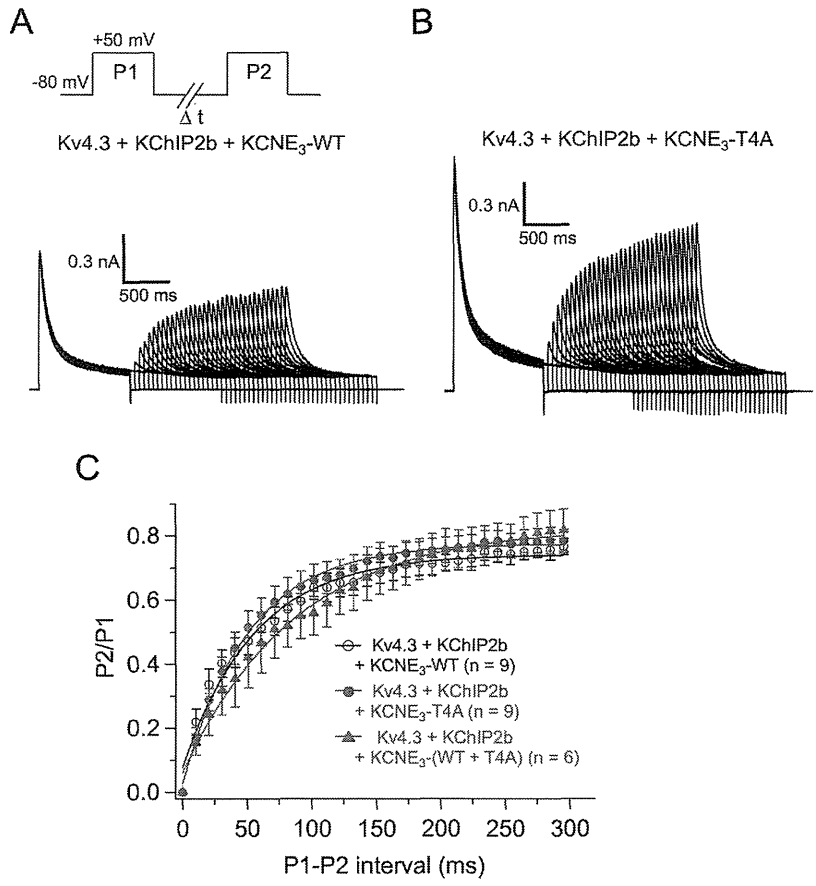

Figure 4. Effects of KCNE3-T4A on recovery from inactivation of the Kv4.3+KChIP2b+KCNE3 channel. A double step-pulse method was used to assess the recovery from inactivation. (**A, inset**) Protocol. A 1-s test pulse to +50 mV (P1) followed by a variable interval at –80 mV, then a second test pulse to +50 mV (P2). (**A,B**) Representative results from cells transfected with (**A**) Kv4.3+KChIP2b+KCNE3-WT and (**B**) Kv4.3+KChIP2b+KCNE3-T4A. (**C**) The time course of recovery of the (open circles) Kv4.3+KChIP2b+KCNE3-WT, (closed circles) KCNE3-T4A, and (filled triangles) KCNE3-(WT+T4A) channels. The ratio to peak current amplitude (P2/P1) is plotted as a function of the inter-pulse (P1–P2) interval.

ics of Kv4.3+KChIP2b+KCNE3 channel, we assessed the current-voltage (I–V) relationship of the Kv4.3+KChIP2b+KCNE3-T4A and Kv4.3+KChIP2b+KCNE3-WT+KCNE3-T4A channels. Coexpression of KCNE3-T4A (at –20 to +50 mV) or KCNE3-WT+KCNE3-T4A (at 0 to +50 mV) significantly increased peak current densities (**Figure 3A**; **Table 2**). Meanwhile, coexpression of KCNE3-T4A, but not KCNE3-(T4A+WT), also caused a negative shift (approximately –5 mV) of voltage dependence of steady-state activation as assessed by plotting the normalized conductance as a function of test potentials (**Figure 3B**; **Table 2**).

Figure 3C shows the representative current traces elicited by a double-step pulse method (inset) used to evaluate steady-state inactivation. Peak currents recorded at various levels of pre-pulse (**Figure 3C**) were normalized by that measured after a 500-ms pre-pulse at –90 mV and plotted as a function of pre-pulse test potentials (**Figure 3D**). Coexpression of KCNE3-T4A or KCNE3-(WT+T4A) with Kv4.3+KChIP2b did not significantly modify the steady-state inactivation of Kv4.3+KChIP2b+KCNE3 channels (**Figure 3D**; **Table 2**).

Because the changes in the time course of reactivation can also affect I_{to} current, a double-pulse protocol (**Figure 4A**) was used to test the effect of KCNE3-T4A or KCNE3-(WT+T4A) coexpression on the time course for recovery from inactivation. **Figures 4A,B** shows the representative current traces for coexpression of KCNE3-WT and KCNE3-T4A. **Figure 4C** shows the time courses of recovery of KCNE3-WT, KCNE3-T4A and KCNE3-(WT+T4A) coexpression together with Kv4.3+KChIP2b. Time constants (τ) of recovery from inactivation are listed in **Table 2**. Coexpression of KCNE3-T4A or KCNE3-(WT+T4A) did not affect the time course of recovery from inactivation.

Phenotype of KCNE3-T4A Mutation in a Simulated Human Right Ventricular Wall Model

To clarify whether the gain of function of I_{to} resulting from KCNE3-T4A mutation is indeed responsible for the Brugada-pattern ECG, we performed computer simulations using the 1-D myocardial model of human right ventricular wall. Based on the I_{to} obtained in electrophysiologic recording (**Figures 3A,B,D**), we numerically reproduced the current-voltage relationship curves (**Figure 5A**), the normalized conductance-voltage relationship curves (**Figure 5B**), and the steady-state inactivation curves (**Figure 5C**) of the KCNE3-WT and KCNE3-T4A channels. The numerically reproduced I_{to} was incorporated into the 1-D right ventricular wall model, consisting of endocardial and epicardial layers (**Figure 5D**). We found that the difference in the phase 2 AP between endocardial and epicardial layers in the KCNE3-T4A model was larger than that in the KCNE3-WT model, and therefore the simulated right precordial ECG showed ST-segment elevation in the case of KCNE3-T4A (**Figure 5E**).

To examine the adequacy of the KCNE3-T4A model, we additionally conducted simulations with sodium channel blockade. In the case of KCNE3-WT (**Figure 5F**), because sodium channel block (I_{Na} 50%) did not increase the difference in phase

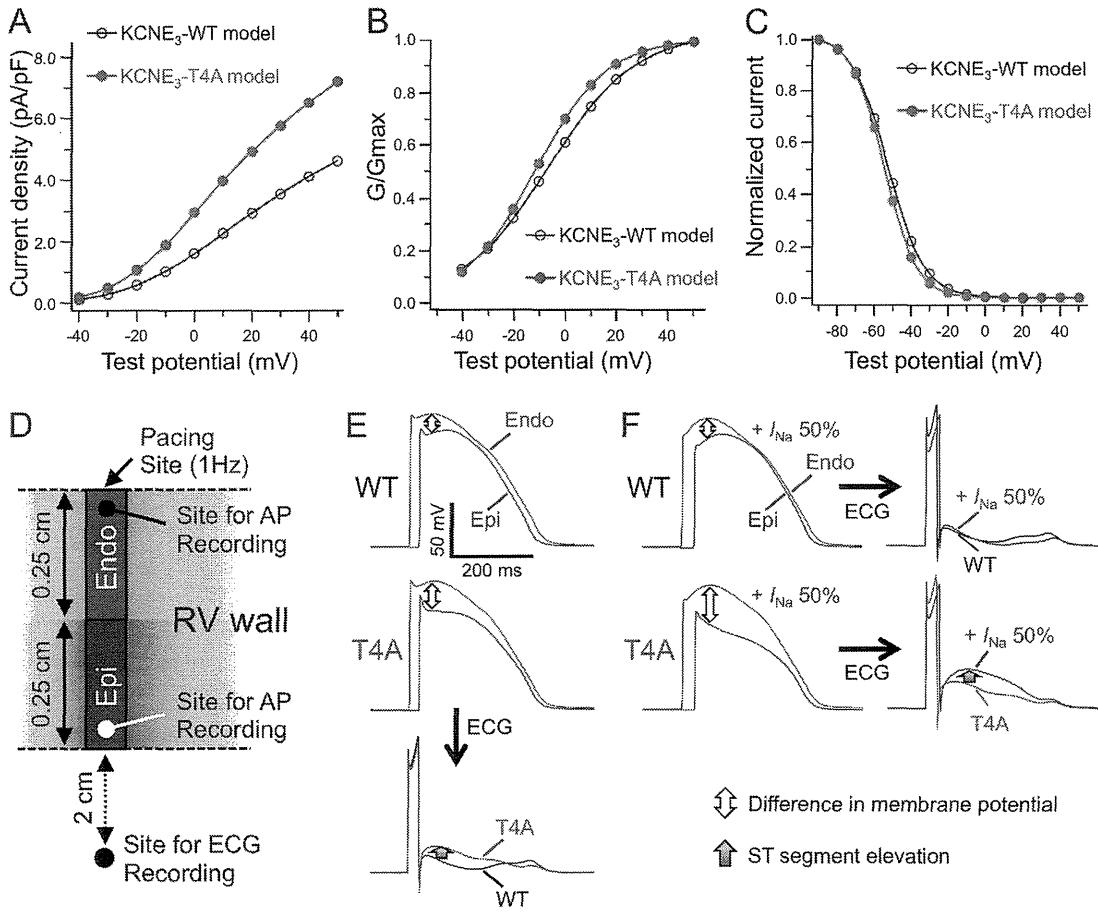

Figure 5. (**A–C**) Numerically reproduced (**A**) current-voltage relationship curves, (**B**) normalized conductance-voltage relationship curves, and (**C**) steady-state inactivation curves of KCNE3-WT and KCNE3-T4A models. (**D**) One-dimensional bidomain myocardial computer model, representing the electrical behaviors of the right ventricular wall. The sites for pacing and recording action potential (AP) and electrocardiogram (ECG) are shown. (**E**) Influence of KCNE3-T4A mutation on both AP and ECG. Endo, endocardial layer; Epi, epicardial layer. (**F**) Effect of sodium channel blockade (I_{Na} 50%) on both AP and ECG in KCNE3-WT and KCNE3-T4A cases.

1 AP between endocardial and epicardial layers, no ST-segment elevation was observed in the simulated ECG. In contrast, in the case of KCNE3-T4A (**Figure 5F**), the same sodium channel block caused the loss of dome of AP in the epicardial layer rather than the endocardial layer, and therefore the simulated ECG showed marked ST-segment elevation, consistent with clinical observation (**Figure 1C**).

Discussion

We identified a *KCNE3* T4A mutation among 40 consecutive patients with Brugada-pattern ECG. The index patient had experienced several episodes of syncope, possibly due to NMS rather than BrS-related ventricular tachyarrhythmias.

The gain of function of I_{to} by mutations in genes that encode I_{to} had been thought to cause BrS.[14,15] Indeed, an R99H mutation in *KCNE3* was recently identified in 1 BrS family.[6] Functional analysis of I_{to} reconstituted by Kv4.3/KCNE3-R99H showed a gain of function of the channel with a dominant-positive effect. Moreover, the mutation was co-segregated with ECG phenotype.[6] Therefore, the mutation underlies the development of BrS. *KCNE3* T4A, the variant identified in the present cohort, could be a candidate for another *KCNE3* mutation that is associated with BrS.

We reconstituted I_{to} by coexpressing Kv4.3 with KCNE3+KChIP2b in CHO cells, and examined the functional consequence of KCNE3-T4A, because KChIP2 associates with Kv4 and increases Kv4 current with the increase of surface expression of Kv4, by facilitating the trafficking of the channel and the kinetic changes that more resemble native I_{to}.[35] KCNE3-T4A also increased I_{to} with a dominant-positive effect. Moreover, computer simulations based on the I_{to} obtained in electrophysiological recordings demonstrated that KCNE3-T4A recapitulated the ECG phenotype in the present case. These results indicate that *KCNE3* T4A could underlie the pathogenesis of Brugada-pattern ECG. Although it may be required to demonstrate a co-segregation of *KCNE3* T4A with ECG phenotype to validate that the *KCNE3* T4A is associated with Brugada-pattern ECG, we unfortunately could not investigate the patient's family members because of lack of consent.

The precise molecular mechanisms of the reverse of KCNE3-induced suppression of Kv4.3 by KCNE3-T4A remain to be elucidated. Delpón et al demonstrated, using coimmunoprecipitation techniques, that KCNE3 coassociates with Kv4.3 in human atrial myocardium and rat ventricular myocardium.[6] In addition, Lundby and Olesen reported that KCNE3 has an inhibitory effect on Kv4.3 independent of the presence of KChIP2 in a heterologous expression system.[20] Therefore, although we recapitulated I_{to} in the presence of KChIP2b, KCNE3-T4A might reverse the KCNE3-induced suppression of Kv4.3 in the absence of KChIP2b, as is the case with KCNE3-R99H reported by Delpón et al.[6] Interestingly, Lundby and Olesen also reported that delayed injection of KCNE3 into *Xenopus* oocytes can almost completely inhibit Kv4.3 current, suggesting that KCNE3 transcription can act as a regulatory mechanism of the Kv4.3 current density.[20] Further studies of the transcription, trafficking and turnover rate of K4.3 channel and channel complexes in the presence or absence of KChIP2b and KCNE3-WT/T4A, would be required to elucidate the mechanisms of the reverse of KCNE3-induced suppression of I_{to} by KCNE3-T4A.

Yokokawa et al reported that 35% of patients with Brugada-pattern ECG had positive responses during the HUT test,[30] demonstrating a high prevalence of NMS among individuals with Brugada-pattern ECG. Although the autonomic nervous system may play an important role in the development of both BrS and NMS, the precise pathophysiological link between BrS and NMS remains to be elucidated. The identification of a novel *SCN5A* Q55X mutation in a patient with Brugada-pattern ECG presenting as NMS and the expression of *SCN5A* in both myocardial cells and intracardiac ganglia raise the possibility of a genetic association between BrS and NMS.[36,37] *KCNE3* (MiRP2) is also expressed in not only the heart but also the central nervous system, and it modulates delayed rectifier currents in mammalian neurons by forming native channel complexes with Kv2.1 and Kv3.1b.[38] Taken together, *KCNE3* T4A may be associated with both phenotypes of BrS and NMS.

In contrast, we have previously reported that *KCNE3* mutations (R99H and T4A) are associated with long QT syndrome (LQTS).[39] A functional analysis of KCNQ1+KCNE3-R99H coexpression demonstrated a reduction of the repolarizing potassium current, thus supporting the proposition that *KCNE3* R99H could be a cause of LQTS. A functional analysis of KCNQ1+KCNE3-T4A, however, could not demonstrate significant functional abnormalities. Regarding the present case, the QTc interval was not prolonged. Therefore, further studies would be necessary to establish the association between *KCNE3* T4A and LQTS. Along with this line, 2 *KCNE3* T4A carriers we previously reported had no apparent spontaneous ST-segment elevation in the right precordial ECG leads.[39] One carrier was a 16-year-old boy, much younger than most affected patients, and another was an old woman. Pharmacological provocation tests were not performed to study whether they had Brugada-pattern ECG.

Conclusions

We identified a *KCNE3* T4A mutation in a Japanese patient with Brugada-pattern ECG presenting as NMS. Its functional consequence was the gain of function of I_{to}, which could underlie the pathogenesis of Brugada-pattern ECG. The data provide novel insight into the genetic basis of Japanese BrS. Further studies are required to clarify whether the *KCNE3* T4A mutation is also associated with NMS and/or LQTS.

Acknowledgments

We thank the patients for their participation in this study. We thank Takako Kobayashi and Yukiyo Tosaka for helping with the genetic analysis. This work was supported, in part, by a Grant-in-Aid for Scientific Research from the Ministry of Education, Culture, Sports, Science and Technology (to T.N. and M.H.). This work was also supported by grants from the Uehara Memorial Foundation and the Ministry of Health, Labor and Welfare of Japan for Clinical Research on Measures for Intractable Diseases (to M.H.), and the National Natural Science Foundation of China (#81273501 to J.W. and W.G.D.).

Disclosures

Conflict of interest to declare: None.

References

1. Chen Q, Kirsch GE, Zhang D, Brugada R, Brugada J, Brugada P, et al. Genetic basis and molecular mechanism for idiopathic ventricular fibrillation. *Nature* 1998; **392:** 293–296.
2. London B, Michalec M, Mehdi H, Zhu X, Kerchner L, Sanyal S, et al. Mutation in glycerol-3-phosphate dehydrogenase 1 like gene (GPD1-L) decreases cardiac Na+ current and causes inherited arrhythmias. *Circulation* 2007; **116:** 2260–2268.
3. Van Norstrand DW, Valdivia CR, Tester DJ, Ueda K, London B, Makielski JC, et al. Molecular and functional characterization of novel glycerol-3-phosphate dehydrogenase 1 like gene (GPD1-L) mutations in sudden infant death syndrome. *Circulation* 2007; **116:** 2253–2259.
4. Antzelevitch C, Pollevick GD, Cordeiro JM, Casis O, Sanguinetti MC, Aizawa Y, et al. Loss-of-function mutations in the cardiac calcium channel underlie a new clinical entity characterized by ST-segment elevation, short QT intervals, and sudden cardiac death. *Circulation* 2007; **115:** 442–449.
5. Watanabe H, Koopmann TT, Le Scouarnec S, Yang T, Ingram CR, Schott JJ, et al. Sodium channel beta1 subunit mutations associated with Brugada syndrome and cardiac conduction disease in humans. *J Clin Invest* 2008; **118:** 2260–2268.
6. Delpón E, Cordeiro JM, Núñez L, Thomsen PE, Guerchicoff A, Pollevick GD, et al. Functional effects of KCNE3 mutation and its role in the development of Brugada syndrome. *Circ Arrhythm Electrophysiol* 2008; **1:** 209–218.
7. Hu D, Barajas-Martinez H, Burashnikov E, Springer M, Wu Y, Varro A, et al. A mutation in the beta 3 subunit of the cardiac sodium channel associated with Brugada ECG phenotype. *Circ Cardiovasc Genet* 2009; **2:** 270–278.
8. Kattygnarath D, Maugenre S, Neyroud N, Balse E, Ichai C, Denjoy I, et al. MOG1: A new susceptibility gene for Brugada syndrome. *Circ Cardiovasc Genet* 2011; **4:** 261–268.
9. Giudicessi JR, Ye D, Tester DJ, Crotti L, Mugione A, Nesterenko VV, et al. Transient outward current (I(to)) gain-of-function mutations in the KCND3-encoded Kv4.3 potassium channel and Brugada syndrome. *Heart Rhythm* 2011; **8:** 1024–1032.
10. Ohno S, Zankov DP, Ding WG, Itoh H, Makiyama T, Doi T, et al. KCNE5 (KCNE1L) variants are novel modulators of Brugada syndrome and idiopathic ventricular fibrillation. *Circ Arrhythm Electrophysiol* 2011; **4:** 352–361.
11. Barajas-Martinez H, Hu D, Ferrer T, Onetti CG, Wu Y, Burashnikov E, et al. Molecular genetic and functional association of Brugada and early repolarization syndromes with S422L missense mutation in KCNJ8. *Heart Rhythm* 2012; **9:** 548–555.
12. Antzelevitch C. Genetic, molecular and cellular mechanisms underlying the J wave syndromes. *Circ J* 2012; **76:** 1054–1065.
13. Nabauer M, Beuckelmann DJ, Uberfuhr P, Steinbeck G. Regional differences in current density and rate-dependent properties of the transient outward current in subepicardial and subendocardial myocytes of human left ventricle. *Circulation* 1996; **93:** 168–177.
14. Yan GX, Antzelevitch C. Cellular basis for the Brugada syndrome and other mechanisms of arrhythmogenesis associated with ST-segment elevation. *Circulation* 1999; **100:** 1660–1666.
15. Antzelevitch C. Brugada syndrome. *Pacing Clin Electrophysiol* 2006; **29:** 1130–1159.
16. Dixon JE, Shi W, Wang HS, McDonald C, Yu H, Wymore RS, et al. Role of the Kv4.3 K+ channel in ventricular muscle: A molecular correlate for the transient outward current. *Circ Res* 1996; **79:** 659–668.
17. Kuo HC, Cheng CF, Clark RB, Lin JJ, Lin JL, Hoshijima M, et al. A defect in the Kv channel-interacting protein 2 (KChIP2) gene leads to a complete loss of I(to) and confers susceptibility to ventricular tachycardia. *Cell* 2001; **107:** 801–813.

18. Decher N, Uyguner O, Scherer CR, Karaman B, Yuksel-Apak M, Busch AE, et al. hKChIP2 is a functional modifier of hKv4.3 potassium channels: Cloning and expression of a short hKChIP2 splice variant. *Cardiovasc Res* 2001; **52:** 255–264.
19. Radicke S, Cotella D, Graf EM, Banse U, Jost N, Varro A, et al. Functional modulation of the transient outward current Ito by KCNE beta-subunits and regional distribution in human non-failing and failing hearts. *Cardiovasc Res* 2006; **71:** 695–703.
20. Lundby A, Olesen SP. KCNE3 is an inhibitory subunit of the Kv4.3 potassium channel. *Biochem Biophys Res Commun* 2006; **346:** 958–967.
21. Radicke S, Cotella D, Graf EM, Ravens U, Wettwer E. Expression and function of dipeptidyl-aminopeptidase-like protein 6 as a putative beta-subunit of human cardiac transient outward current encoded by Kv4.3. *J Physiol* 2005; **565:** 751–756.
22. Aimond F, Kwak SP, Rhodes KJ, Nerbonne JM. Accessory Kvbeta1 subunits differentially modulate the functional expression of voltage-gated K+ channels in mouse ventricular myocytes. *Circ Res* 2005; **96:** 451–458.
23. Niwa N, Nerbonne JM. Molecular determinants of cardiac transient outward potassium current (I(to)) expression and regulation. *J Mol Cell Cardiol* 2010; **48:** 12–25.
24. Wu J, Shimizu W, Ding WG, Ohno S, Toyoda F, Itoh H, et al. KCNE2 modulation of Kv4.3 current and its potential role in fatal rhythm disorders. *Heart Rhythm* 2010; **7:** 199–205.
25. Nakajima T, Kaneko Y, Saito A, Irie T, Tange S, Iso T, et al. Identification of six novel SCN5A mutations in Japanese patients with Brugada syndrome. *Int Heart J* 2011; **52:** 27–31.
26. Ogawa R, Kishi R, Takagi A, Sakaue I, Takahashi H, Matsumoto N, et al. A novel microsatellite polymorphism of sodium channel beta1-subunit gene (SCN1B) may underlie abnormal cardiac excitation manifested by coved-type ST-elevation compatible with Brugada syndrome in Japanese. *Int J Clin Pharmacol Ther* 2010; **48:** 109–119.
27. Makiyama T, Akao M, Haruna Y, Tsuji K, Doi T, Ohno S, et al. Mutation analysis of the glycerol-3 phosphate dehydrogenase-1 like (GPD1L) gene in Japanese patients with Brugada syndrome. *Circ J* 2008; **72:** 1705–1706.
28. Shimizu A. Is this a philosophic issue? Do patients with drug-induced Brugada type ECG have poor prognosis? (Pro) *Circ J* 2010; **74:** 2455–2463.
29. Nishizaki M, Sakurada H, Yamawake N, Ueda-Tatsumoto A, Hiraoka M. Low risk for arrhythmic events in asymptomatic patients with drug-induced type 1 ECG. Do patients with drug-induced Brugada type ECG have poor prognosis? (Con) *Circ J* 2010; **74:** 2464–2473.
30. Yokokawa M, Okamura H, Noda T, Satomi K, Suyama K, Kurita T, et al. Neurally mediated syncope as a cause of syncope in patients with Brugada electrocardiogram. *J Cardiovasc Electrophysiol* 2010; **21:** 186–192.
31. Nakajima T, Kaneko Y, Irie T, Takahashi R, Kato T, Iijima T, et al. Compound and digenic heterozygosity in desmosome genes as a cause of arrhythmogenic right ventricular cardiomyopathy in Japanese patients. *Circ J* 2012; **76:** 737–743.
32. Priebe L, Beuckelmann DJ. Simulation study of cellular electric properties in heart failure. *Circ Res* 1998; **82:** 1206–1223.
33. Tsuji-Wakisaka K, Akao M, Ishii TM, Ashihara T, Makiyama T, Ohno S, et al. Identification and functional characterization of KCNQ1 mutations around the exon 7-intron 7 junction affecting the splicing process. *Biochim Biophys Acta* 2011; **1812:** 1452–1459.
34. Wang S, Bondarenko VE, Qu Y, Morales MJ, Rasmusson RL, Strauss HC. Activation properties of Kv4.3 channels: Time, voltage and [K+]o dependence. *J Physiol* 2004; **557:** 705–717.
35. An WF, Bowlby MR, Betty M, Cao J, Ling HP, Mendoza G, et al. Modulation of A-type potassium channels by a family of calcium sensors. *Nature* 2000; **403:** 553–556.
36. Makita N, Sumitomo N, Watanabe I, Tsutsui H. Novel SCN5A mutation (Q55X) associated with age-dependent expression of Brugada syndrome presenting as neurally mediated syncope. *Heart Rhythm* 2007; **4:** 516–519.
37. Scornik FS, Desai M, Brugada R, Guerchicoff A, Pollevick GD, Antzelevitch C, et al. Functional expression of "cardiac-type" Nav1.5 sodium channel in canine intracardiac ganglia. *Heart Rhythm* 2006; **3:** 842–850.
38. McCrossan ZA, Lewis A, Panaghie G, Jordan PN, Christini DJ, Lerner DJ, et al. MinK-related peptide 2 modulates Kv2.1 and Kv3.1 potassium channels in mammalian brain. *J Neurosci* 2003; **23:** 8077–8091.
39. Ohno S, Toyoda F, Zankov DP, Yoshida H, Makiyama T, Tsuji K, et al. Novel KCNE3 mutation reduces repolarizing potassium current and associated with long QT syndrome. *Hum Mutat* 2009; **30:** 557–563.

Circulation Journal
Official Journal of the Japanese Circulation Society
http://www.j-circ.or.jp

ORIGINAL ARTICLE
Arrhythmia/Electrophysiology

Seasonal and Circadian Distributions of Cardiac Events in Genotyped Patients With Congenital Long QT Syndrome

Masateru Takigawa, MD; Mihoko Kawamura, MD; Takashi Noda, MD, PhD; Yuko Yamada, MD; Koji Miyamoto, MD; Hideo Okamura, MD; Kazuhiro Satomi, MD, PhD; Takeshi Aiba, MD, PhD; Shiro Kamakura, MD, PhD; Tomoko Sakaguchi, MD, PhD; Yuka Mizusawa, MD; Hideki Itoh, MD, PhD; Minoru Horie, MD, PhD; Wataru Shimizu, MD, PhD

Background: Although the incidence of ventricular tachyarrhythmias associated with structural heart disease is highest in winter and during the daytime, seasonal and circadian variations among cardiac events in patients with congenital long QT syndrome (LQTS) remain unknown. The present study aims to determine seasonal and circadian cardiac events in patients with a congenital LQTS genotype.

Methods and Results: The medical records of 196 consecutive patients with symptomatic LQTS (age, 32±19 years; female, n=133; LQT1, n=86; LQT2, n=95; LQT3, n=15) who were genotyped between 1979 and 2006 at 2 major Japanese institutions were retrospectively analyzed. The patients with LQT1, LQT2, and LQT3 developed 223,550 and 59 cardiac events during a mean follow-up of 26, 33, and 25 years, respectively. The numbers of cardiac events significantly peaked during the summer among those with LQT1 (P<0.001) and from summer to fall in those with LQT2 (P<0.001), but reached the nadir in winter among those with LQT3 (P=0.003). Cardiac events significantly peaked in the afternoon (12:00–17:59) and morning (06:00–11:59) among those with LQT1 (P<0.001) and LQT2 (P<0.001).

Conclusions: The frequency of cardiac events was specifically seasonal and circadian among patients with the 3 major genotypes of congenital LQTS. (*Circ J* 2012; **76:** 2112–2118)

Key Words: Cardiac events; Circadian; Long QT syndrome; Seasonal

Congenital long-QT syndrome (LQTS) is caused by mutations in genes encoding channels that regulate potassium, sodium, or calcium currents, and by mutations in a cytoskeletal gene that affects sodium and calcium kinetics, resulting in prolonged ventricular repolarization and an increased risk for sustained ventricular tachyarrhythmias.[1] Although the incidence of ventricular tachyarrhythmias including ventricular tachycardia (VT) and ventricular fibrillation (VF) is the highest in winter and during the daytime among patients with structural heart disease,[2–9] the seasonal and circadian occurrence of cardiac events as a result of torsade de pointes remains unknown in patients with congenital LQTS.

We analyzed the medical records of patients genotyped with congenital LQTS to determine the seasonal and circadian occurrence of cardiac events.

Methods

Study Population

The present study included 196 (age, 32±19 years; female, n=133) consecutive patients with symptomatic LQTS and detailed medical information who were genotyped at 2 major Japanese institutions (National Cerebral and Cardiovascular Center, Suita, and Shiga University of Medical Science, Ohtsu)

Received February 21, 2012; revised manuscript received April 28, 2012; accepted May 22, 2012; released online June 23, 2012 Time for primary review: 7 days

Division of Arrhythmia and Electrophysiology, Department of Cardiovascular Medicine, National Cerebral and Cardiovascular Center, Suita (M.T., T.N., Y.Y., K.M., H.O., K.S., T.A., S.K., W.S.); Department of Cardiovascular and Respiratory Medicine, Shiga University of Medical Science, Ohtsu (M.K., T.S., Y.M., H.I., M.H.), Japan

The first two authors contributed equally (M.T., M.K.).

Presented in part at the Heart Rhythm 2009, Boston, Massachusetts, USA, May 13-16, 2009, and published in abstract form (Heart Rhythm. 2009; May, S162).

Current address: Cardiovascular Center, Department of Internal Medicine, Yokosuka Kyosai Hospital, Yokosuka, Kanagawa, Japan (M.T.).

Mailing address: Wataru Shimizu, MD, PhD, Division of Arrhythmia and Electrophysiology, Department of Cardiovascular Medicine, National Cerebral and Cardiovascular Center, 5-7-1 Fujishiro-dai, Suita 565-8565, Japan. E-mail: wshimizu@hsp.ncvc.go.jp

ISSN-1346-9843 doi:10.1253/circj.CJ-12-0213

Table 1. Baseline Characteristics of the Study Population (n=196)

	LQT1	LQT2	LQT3	Total
Patients	86	95	15	196
Gender, female	60 (69.8%)	67 (70.5%)	6 (40.0%)	133 (67.9%)
Age at the study (follow-up)	25.8±14.1	32.5±14.8	25.3±18.1	28.0±15.6
Age at the genetic test	15.5±15.6	26.9±13.9	18.8±13.7	20.6±15.2
β-blockers	59 (68.6%)	62 (65.3%)	6 (40.0%)	127 (64.8%)
ICD therapy	9 (10.5%)	16 (16.8%)	5 (33.3%)	30 (15.3%)
Total cardiac events	223	550	59	832
Mean events number/patient	2.6±2.7	5.8±11.5	3.9±4.9	4.2±8.5
Median/range events	2 (1–18)	3 (1–75)	2 (1–19)	2 (1–75)

LQT, Long QT; ICD, implantable cardioverter defibrillator.

Table 2. Details of Cardiac Events in Each Type of LQT Syndrome

	Presyncope	Syncope	Cardiac arrest or death	Total cardiac events
LQT1	16 (7.2%)	190 (85.2%)	17 (7.6%)	223
LQT2	220 (40.0%)	311 (56.5%)	19 (3.5%)	550
LQT3	2 (3.4%)	35 (59.3%)	22 (37.3%)	59

LQT, Long QT.

between 1979 and 2006. Eighty-six, 95, and 15 patients had LQT1, LQT2, and LQT3, respectively. The LQTS patients having compound mutations or other mutations except for LQT1, LQT2, and LQT3 were excluded from the analysis. Symptoms included presyncope, syncope, and cardiac arrest. Sudden dizziness, palpitation, and chest pain persisting for over 30 s without a complete loss of consciousness confirmed by electrocardiogram (ECG) recordings as being associated with ventricular tachyarrhythmias at least once were included as presyncope. Multiple events were defined as over 2 cardiac events per 24-h period. Written informed consent was obtained from each patient in this study to undergo genetic testing. The privacy of the patients was protected by the anonymization of all data.

Data Collection

In general, the LQTS patients were first referred to our hospital or to a local outpatient clinic for evaluation and therapy, and followed up routinely every 1–3 months. After genotyping at our hospital, they attended our outpatient clinic every 1–6 months (mean, 2.2±1.1 months; median, 2 months). The follow-up period included all periods since the first presentation at our hospital or a local outpatient clinic. A detailed history was obtained at each visit and all patients were encouraged to attend the clinic whenever they experienced palpitations, chest pain, presyncope, or syncope. Patients with cardiac arrest were usually conveyed to our hospital. We obtained as complete a medical history as possible from patients and their relatives, and retrospectively analyzed these records in detail to determine the seasonal and circadian distribution of cardiac events. Some patients were followed up at other outpatient clinics even after genetic testing when they lived far from our institutions. Local physicians or pediatric cardiologists then provided detailed information taken directly from their own medical records, as well as from the patients and their families.

Seasons are defined in the present study according to the Japanese calendar as winter, December to February; spring, March to May; summer, June to August; and fall, September to November. The time of day was classified as night-time (00:00–05:59), morning (06:00–11:59), afternoon (12:00–17:59), and evening (18:00–23:59). Triggers of cardiac events were classified as exercise, emotion, and rest or sleep without arousal according to a previous report.[10]

Statistics

Quantitative data are presented as means±SD or medians/range, and were compared using ANOVA or Kruskal-Wallis analysis. Categorical data are presented as absolute and percentage frequencies, and were analyzed using the χ^2 test. The difference in the frequency of cardiac events was analyzed using the goodness-of-fit test for multinomial distribution. A value of $P<0.05$ was considered significant.

Results

Patient Characteristics

The baseline characteristics of the study population are shown in Table 1. Females comprised about 70% of the LQT1 and LQT2 groups but only 40% of the LQT3 group. The total numbers of cardiac events were 223, 550, and 59 in the LQT1, LQT2, and LQT3 groups during a mean follow-up of 26, 33, and 25 years, respectively. The numbers of events per genotype significantly differed (P=0.007), being 2.6, 5.8, and 3.9 in the LQT1, LQT2, and LQT3 groups, respectively. Table 2 shows details of the cardiac events that occurred in each LQTS type. The frequency of more severe symptoms of cardiac events, such as syncope, cardiac arrest, and sudden death, were higher in the LQT1 and LQT3 groups than in the LQT2 group, in which such extreme symptoms accounted for 60% of the total number of events. Symptoms such as presyncope were milder in the remaining 40% of the LQT2 group.

Seasonal and Circadian Distribution of Cardiac Events in LQT1

Among a total of 223 cardiac events, details about the season and time of occurrence for 42 (18.8%) and 55 (24.7%) events, respectively, were vague. Among 181 (81.2%) events with de-

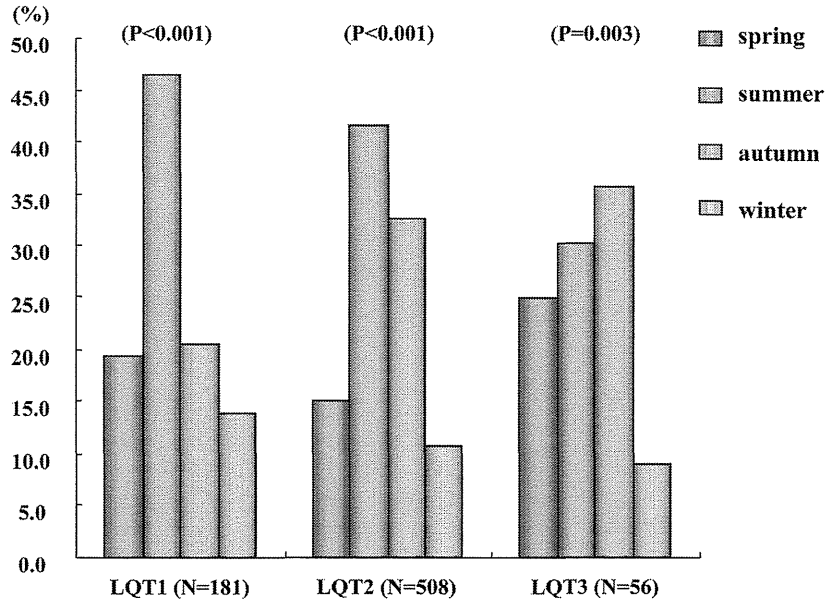

Figure 1. Bar graphs showing the seasonal distribution in occurrence of cardiac events in each genotype of congenital long QT syndrome (LQTS). Detailed seasonal information was acquired in 181/223 (81.2%), 508/550 (92.4%), and 56/59 (94.9%), in LQT1, LQT2, and LQT3, respectively.

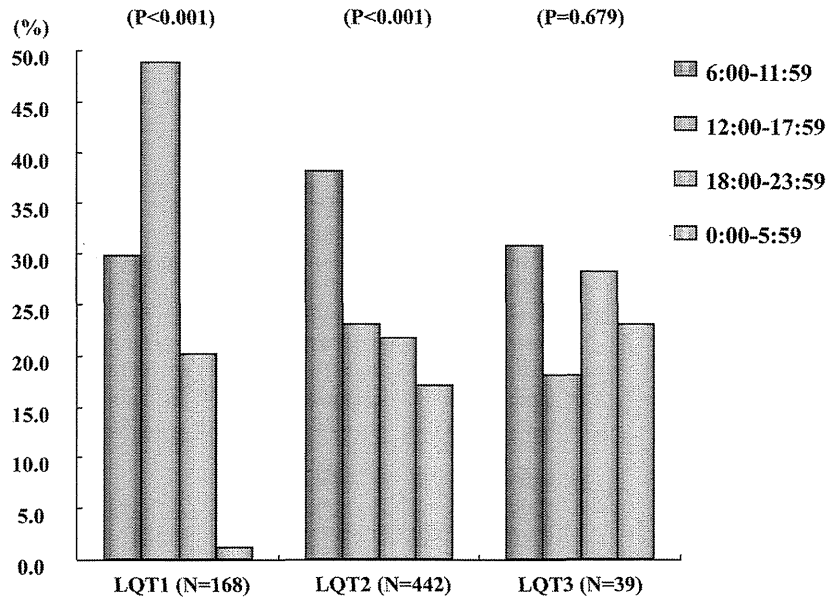

Figure 2. Bar graphs showing the circadian distribution in occurrence of cardiac events in each genotype of congenital long QT syndrome (LQTS). Detailed circadian information was acquired in 168/223 (75.3%), 442/550 (80.4%), and 39/59 (66.1%), in LQT1, LQT2, and LQT3, respectively.

tailed seasonal information, most occurred during the summer (84/181, 46.4%) and the frequency was lowest during the winter (25/181, 13.8%) (**Figure 1**). Among 168 (75.3%) events with detailed time information, the frequency was highest during the afternoon (82/168, 48.8%), followed by the morning (50/168, 29.8%), and lowest during the night-time (2/168, 1.2%) (**Figure 2**). Among the 50 events that occurred during the morning, extremely few arose at the time of awakening. Only 5 (10%) occurred during first 2 h of the morning (6:00–7:59) (P<0.001), and the remaining 45 (90%) events occurred during the late morning (8:00–11:59). Both the seasonal incidence of cardiac events among 3-month periods and the circadian incidence among 6-h periods statistically differed (both, P<0.001).

Seasonal and Circadian Distribution of Cardiac Events in LQT2

Among a total of 550 cardiac events, details about the season and time of occurrence were vague for 42 (7.6%) and 108 (19.6%) events, respectively. Among 508 (92.4%) cardiac events with detailed seasonal information, the frequency was highest during the summer (211/508, 41.5%), followed by the fall (166/508, 32.7%), and lowest during the winter (55/508, 10.8%) (**Figure 1**). Among 442 (80.4%) cardiac events with

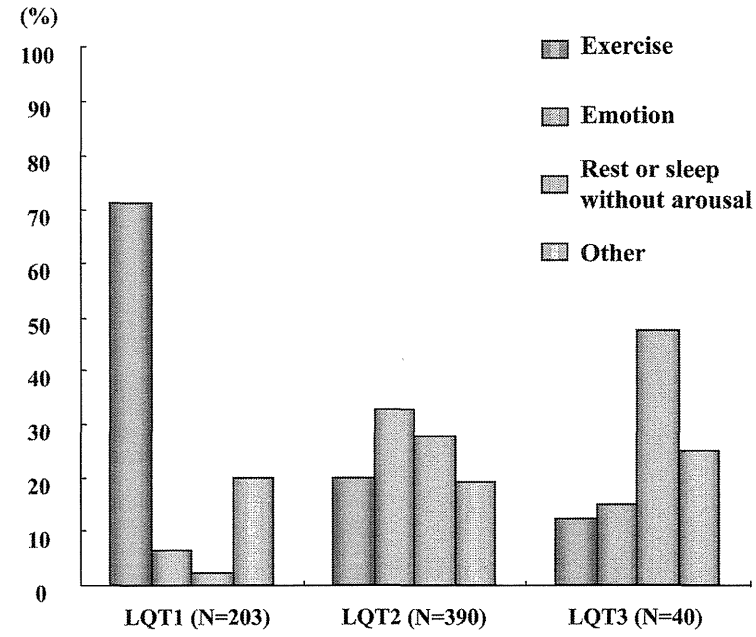

Figure 3. The frequency of 4 different factors triggering cardiac events are indicated as bar graphs. Detailed trigger was acquired in 203/223 (91.0%), 390/550 (70.9%), and 40/59 (67.8%), in LQT1, LQT2, and LQT3, respectively.

detailed time information, the frequency was highest during the morning (169/442, 38.2%), followed by the afternoon (102/442, 23.1%), and evening (96/442, 21.7%) (Figure 2), and lowest during the night-time (75/442, 17.0%) (Figure 2). Cardiac events associated with the morning were concentrated within the first 2 h of awakening (89/169, 52.7%) between 6:00 and 7:59 (P<0.001). Both the seasonal incidence of cardiac events among the 3-month periods and the circadian incidence among the 6-h periods statistically differed (both, P<0.001).

Seasonal and Circadian Distribution of Cardiac Events in LQT3

Among a total of 59 cardiac events, details about the season and time of occurrence were vague for 3 (5.1%) and 20 (33.9%) events, respectively. Among 56 (94.9%) events with detailed seasonal information, the frequency was the highest during the fall (20/56, 35.7%), followed by summer (17/56, 30.4%), and spring (14/56, 25.0%), and lowest during the winter (5/56, 8.9%) (Figure 1). Among 39 (66.1%) events with detailed time information, the frequency of cardiac events was highest at midnight in LQT3 compared with LQT1 and LQT2 (Figure 2). The seasonal incidence of cardiac events among the 3-month periods statistically differed (P=0.003), whereas the circadian incidence among the 6-h periods did not (P=0.679).

Triggers of Cardiac Events in LQTS

Figure 3 shows triggers for cardiac events. Triggers were confirmed in 203 (91.0%), 390 (70.9%), and 40 (67.8%) events in LQT1, LQT2, and LQT3, respectively. Most cardiac events in the LQT1 group developed during exercise (144/203, 70.9%), although fewer events occurred during emotional stress (13/203, 6.4%) or rest (5/203, 2.5%). Among 144 cardiac events caused by exertion, 39 (27.1%) were associated with swimming, which accounted for 52% of the triggers of cardiac events during summer exertion. No typical trigger was identified among patients with LQT2, although relatively more cardiac events developed in this group during emotional stress (128/390, 32.8%), such as arousal or being startled by the sudden ringing of a telephone or a bell, and psychological stress including fear, anxiety, and anger, and fewer developed during rest or sleep without arousal (109/390, 27.9%) or exercise (78/390, 20.0%). In addition, the features of exercise as a trigger for LQT2 were unlike those of LQT1 insofar as they were considerably milder and included routine activities such as standing from a seated position, walking, and brushing teeth. In addition, events tended to occur at the start of such activities in the LQT2 group compared with during more intense exercise in the LQT1 group. Cardiac events were more frequent during rest or sleep without arousal in the LQT3 group (19/40, 47.5%) compared with exercise (5/40, 12.5%) and emotional stress (6/40, 15.0%).

Seasonal Distribution of Multiple Events

Multiple events occurred within 24 h in 13/86 (15.1%), 30/95 (31.6%), and 4/15 (26.7%) patients with LQT1, LQT2, and LQT3, respectively. Among a total of 13 multiple events in the patients with LQT1, 2 (15.4%), 5 (38.5%), 5 (38.5%), and 1 (7.7%) occurred during the spring, summer, fall, and winter, respectively. Among a total of 55 multiple events in the LQT2 group, 3 (5.5%), 27 (49.1%), 22 (40%), and 3 (5.5%) events occurred during these respective seasons. Among a total of 4 multiple events that occurred in the LQT3 group, 2 (50.0%) occurred during the spring, 1 (25.0%) occurred during the summer, and 1 (25.0%) occurred during the winter. The seasonal distribution was significant in both the LQT1 and LQT2 groups, but was difficult to analyze in the LQT3 group because relatively few total events occurred. Over 75% and about 90% of multiple events in LQT1 and LQT2 occurred between summer and fall.

Discussion

Although several investigators have examined the seasonal or